Title: Novel zinc attenuating compounds as potent broad spectrum antifungal agents with *in vitro* and *in vivo* efficacy.

Authors: Karen A. O'Hanlon Cohrt[1], Laura Marín[2], Lasse Kjellerup[1,3], Johannes D. Clausen[1], William Dalby-Brown[1], José Antonio Calera[4], Anne-Marie Lund Winther[1].

[1]Pcovery, Ole Maaløes vej 3, 2200 Copenhagen N, Denmark

[2]Instituto de Biología Funcional y Genómica (IBFG). Consejo Superior de Investigaciones Científicas (CSIC). Salamanca, Spain

[3]Department of Plant and Environmental Sciences, University of Copenhagen, DK-1871 Frederiksberg, Denmark

[4]Instituto de Biología Funcional y Genómica (IBFG). Departamento de Microbiología y Genética, Universidad de Salamanca. Salamanca, Spain

Running title: Antifungal zinc attenuating compounds

Correspondence: Anne-Marie Lund Winther, Phone: +4551594561, Mail: amw@pcovery.com.

Keywords: zinc homeostasis, yeast, antifungal, zinc deprivation

Abstract

An increase in the incidence of rare but hard-to-treat invasive fungal pathogens as well as resistance to the currently available antifungal drugs calls for new broad-spectrum antifungals with a novel mechanism of action. Here, we report the identification and characterization of two novel zinc-attenuating compounds ZAC307 and ZAC989, which exhibit broad-spectrum *in vitro* antifungal activity and *in vivo* efficacy in a fungal kidney burden candidiasis model.

The compounds were identified serendipitously as part of a drug discovery process aimed at finding novel inhibitors of the fungal plasma membrane proton ATPase, Pma1. Based on their structure, we hypothesized that they might act as zinc chelators. Indeed, both fluorescence-based affinity determination and potentiometric assays revealed these compounds, subsequently termed zinc attenuating compounds (ZACs), to have strong affinity for zinc, and their growth inhibitory effects on *Candida albicans* and *Aspergillus fumigatus* could be inactivated by the addition of exogenous zinc to fungal growth media. We determined the ZACs to be fungistatic, with a low propensity for resistance development. Gene expression analysis suggested that the ZACs interfere negatively with the expression of genes encoding the major components of the *A. fumigatus* zinc uptake system, thus supporting perturbance of zinc homeostasis as the likely mode of action. Taken together, with demonstrated *in vitro* and *in vivo* antifungal activity, low propensity for resistance development, and a novel mode of action, the ZACs represent a promising new class of antifungal compounds, and their advancement in a drug development program is therefore warranted.

Introduction

The success of pathogenic microorganisms hinges upon their ability to sequester essential nutrients from their host during infection. Through a process known as nutritional immunity, the host immune system sequesters metals that are necessary for microbial growth, resulting in an extremely nutrient-limited host environment (1). For example, vertebrates express a number of iron-binding molecules, e.g., the transferrin family, that ensure extremely low concentrations of free iron in the body (2). Additionally, neutrophils and other myeloid and non-myeloid cells synthesize large amounts of the antimicrobial Zn^{2+}/Mn^{2+}-chelating protein calprotectin during infection, and the contribution of calprotectin to the innate immune response against yeast and filamentous fungal pathogens is well documented (3–5).

For fungal pathogens to grow and establish infection inside their host, they must be able to obtain iron, zinc, and other essential metals from the harsh environment imposed by nutritional immunity (6). Consequently, successful pathogens have evolved elegant mechanisms to sequester essential metals from their hosts during infection. The mechanisms for iron sequestration are best described, and include the expression of high affinity iron transporters, iron-chelating siderophores and iron-binding proteins (1, 7, 8). Although iron acquisition is recognized as a virulence factor for many fungal pathogens (7), research in recent years has highlighted the important contribution that zinc sequestration makes to fungal pathogenesis and virulence (4, 9). Indeed, fungal acquisition of zinc has been clearly demonstrated to be essential for fungal growth and pathogenicity and zinc-depleting conditions are known to reduce fungal growth *in vitro* (3, 10, 11).

In all fungal species, the major zinc-binding proteins include Cu^{2+}/Zn^{2+} superoxide dismutases (SODs), alcohol dehydrogenase and ribosomal proteins (12). SODs are key enzymes in fungal virulence and are necessary for the detoxification of reactive oxygen species generated by host cells

during fungal infection (13). In *A. fumigatus*, zinc uptake is regulated by the transcriptional regulator ZafA, and deletion of *zafA* has been shown to not only impair germination and overall growth capacity of *A. fumigatus* in zinc-limiting media, but it also completely abrogates *A. fumigatus* virulence in a murine model of invasive aspergillosis (11). Thus, the control of access to zinc is one of the central battlefields on which the outcome of an infection is decided. In further support of this notion, calprotectin comprises ~40% of total protein content in the neutrophil cytoplasm during infection, and its antifungal effect can be reversed *in vitro* by micromolar quantities of zinc (3, 4, 9). Because of the great need for fungal zinc uptake during infection, it has been hypothesized that both chelation therapy and the modulation of zinc homeostasis and zinc acquisition are promising antifungal strategies (14–18).

We have previously reported the identification of novel antifungal compounds targeting the fungal plasma membrane H^+-ATPase (19, 20). In the further optimization process a number of compounds were synthesized, and we found two of these compounds, ZAC307 and ZAC989, to be very potent inhibitors of *Candida albicans* growth, despite the fact that they lacked H^+-ATPase inhibitory activity. Due to their characteristic arrangement of an aromatic structure with nitrogen bound in close proximity to a hydroxyl group, we speculated that ZAC307 and ZAC989 could act as metal chelators. Thus, the goals of this study were: i) to investigate the chelating properties of these compounds; ii) to characterize the spectrum of antifungal activity of these compounds *in vitro*; iii) to ascertain whether the compounds were fungistatic or fungicidal, and the propensity of *C. albicans* to develop resistance against these compounds; iv) to investigate whether the antifungal activity was caused by extracellular zinc sequestration or if the compounds were taken up by *Candida albicans* cells; v) to assess whether or not these compounds influenced the expression level of genes encoding zinc transporters required for zinc uptake from zinc-limiting media and that of

other genes regulated by ZafA, which is the master regulator of zinc homeostasis in *Aspergillus fumigatus*, and vi) to test and evaluate the effects of these compounds against mammalian cells and their antifungal efficacy *in vivo* in a murine model of candidiasis.

Results

ZAC307 and ZAC989 have high binding affinity for zinc and copper, but not for magnesium and calcium

ZAC307, ZAC989, ZAC623 (collectively referred to as ZACs) and the reference compounds EDTA and TPEN (Fig. 1) were evaluated for their zinc binding properties. ZAC307 and ZAC989 have dissociation constants (K_D) in the low nanomolar range (K_D = 13 – 71 nM), as determined by a fluorescence-based competition assay (Table 1). ZAC623 exhibited poor affinity for zinc, with a dissociation constant > 6 µM. Dissociation constants for EDTA and TPEN could not be determined with this assay as their dissociation constants were below the measurable range, but both have previously been reported to be very potent zinc chelators (21).

The Zn^{2+}-binding properties of ZAC307 and ZAC989 were further evaluated using a potentiometric assay, where pH is measured as a function of base (NaOH) added to the compound, either in the absence or presence of metal. Since potentiometric methods require millimolar concentrations, and ZAC307 and ZAC989 displayed poor solubility in water at such high concentrations, the measurements were performed in a mixture of DMSO/water (70:30 v/v), as described previously (22). To determine the deprotonation constant, a solution of 1 mM ZAC307 or ZAC989 was titrated with 0.3 M NaOH at constant ionic strength (Fig. 2A and 2B). In a second run, the same titration was performed in the presence of 0.5 equivalents of Zn^{2+} for ZAC307 and ZAC989. A shift in the pH curve in the presence of the metal (Fig 2A: ZAC307, 0.5eq Zn^{2+}) as compared to the absence of the metal (Fig 2A: ZAC307) indicates binding of the Zn^{2+} to the compound. The measured pH data

were analyzed with the Hyperquad program suite, taking into account all relevant equilibrium constants, including also the constants for metal hydroxylation. The analysis provides the pK_a values and metal complex stability constants, as well as a speciation calculation, indicating how many ZAC molecules are involved in coordinating the Zn^{2+} ion at different pH values. Refinement of the measured pH data for ZAC307 provided a pK_a value of 6.84, and formation constants log β_1, log β_2, and log β_3 of 7.47, 13.27, and 18.14, corresponding to the formation of a 1:1, 2:1, and 3:1 ligand-Zn(II) complex, respectively. The corresponding species distribution diagram is displayed in Fig. 2C and this shows that, at neutral pH in a DMSO/water solvent mixture, the ligand-zinc stoichiometry is a mixture of 1:1, 2:1 and 3:1 binding, with 2:1 and 3:1 being the dominant stoichiometries. Similar potentiometric experiments were carried out with $CaCl_2$ and $MgCl_2$ in place of $Zn(NO_3)_2$, and these revealed that Ca^{2+} and Mg^{2+} binding to ZAC307 is negligible (Fig. 2A). Potentiometric titration of ZAC307 with $CuSO_4$ was not possible due to precipitation of the resulting complex suggesting that ZAC307 also binds copper. Refinement of the measured pH data for ZAC989 provided a pK_a value of 7.70, and in the presence of zinc we measured formation constants log β_1, log β_2, and log β_3 of 7.35, 14.30, and 19.71, corresponding to the formation of a 1:1, 2:1, and 3:1 ligand-Zn(II) complex, respectively (Fig. 2D). Potentiometric experiments were also carried out with ZAC989 and $CuSO_4$, $CaCl_2$ and $MgCl_2$, and the data indicated that ZAC989 chelates copper, whereas binding of calcium and magnesium is negligible. ZAC989 bound copper with the formation constants log β_1, log β_2, and log β_3 of 7.83, 13.37, and 20.62, respectively. The most dominant ZAC989-copper stoichiometry was a 3:1 stoichiometry (Fig. 2E).

ZACs are potent broad-spectrum fungistatic yeast inhibitors that work intracellularly and display low potential for resistance development

ZAC307 and ZAC989 exhibit antifungal activity, and display potent growth inhibition in the low µg/mL range (0.2 – 0.9 µg/mL) against a number of pathogenic *Candida* species, including a *Candida glabrata* strain with increased efflux pump activity (Table 2). The minimum inhibitory concentration (MIC) was defined as the lowest compound concentration that resulted in at least 50% growth inhibition for yeasts, which corresponded to a prominent decrease in visible growth. For molds the MIC was defined as the lowest concentration of the compound that resulted in no visible growth. In *Candida albicans* this value was 0.6 µg/mL for ZAC989 and 0.4 µg/mL for ZAC989. ZAC623 did not display growth inhibitory activity against *C. albicans* (Fig. 3A). The known potent metal chelators EDTA and TPEN both exhibited a MIC of ~0.05 µg/mL, but TPEN led to a more complete growth inhibition as compared to EDTA (Fig. 3B). The antifungal effects of ZAC989 and ZAC307 were reversed by exogenous addition of zinc or copper to the growth medium in the presence of either ZAC989 or ZAC307 (Fig. 3C and 3D). Zinc ions were most effective in reversing the growth inhibitory effects of the ZACs, with restoration of fungal growth observed in the presence of 1 µM Zn^{2+}. Addition of iron (Fe^{2+}) had a modest effect on the antifungal activity of ZAC989 and ZAC307, with a fungal growth rate of approximately 50% in the presence of 100 µM Fe^{2+} as compared to control cells. In accordance with the results obtained from potentiometric titration, the addition of magnesium or calcium had no effect on the antifungal activity of the ZACs (Fig. 3C and 3D).

Time-kill investigations revealed that the ZACs exhibited fungistatic activity against *C. albicans* in contrast to amphotericin B (AMB), which exhibits fungicidal activity after 3 h of exposure (Fig. 4A). Both EDTA and TPEN exhibited a fungistatic effect within the first 24 h of exposure. Fungal growth recovery was evaluated after longer exposure times of *C. albicans* cells to the ZACs. This revealed that the fungal cells were able to resume growth when moved to fresh growth media in the absence of ZACs (Fig. 4B). Fungal cells exposed to TPEN at concentrations above 2 µg/mL

showed poor recovery and this may be explained by the strong chelating properties of TPEN that enable it to extract zinc from essential enzymes leading to fungal cell death after prolonged exposure (Fig. 4C).

In order to gain an understanding of the potential of ZACs to permeabilize into fungal cells, we monitored the intracellular zinc levels of *C. albicans* cells that were exposed to TPEN, EDTA or ZACs using the cell-permeable fluorescent probe zinbo-5. The affinity constant of this probe for zinc is 2.2 nM (23), which is weaker than that of most zinc-binding proteins, and thus it only reports the free or weakly bound zinc ions. The probe localizes to the internal membrane system including the ER in *C. albicans* (L. Kjellerup, A. L. Winther, D. Wilson, and A. T. Fuglsang, submitted for publication). A decreased zinbo-5-fluorescent signal in the presence of fungal cells, compound and zinc would indicate that intracellular zinbo-5 is competing with the added compound for zinc ions. ZAC307 and ZAC989 were evaluated at a concentration of 25 µM, equivalent to 7 µg/mL and 9 µg/mL respectively. ZAC989 induced a time-dependent decrease in zinbo-5 fluorescence, similarly to 1.3 µg/mL TPEN (Fig. 4D). ZAC307 decreased the zinbo-5 fluorescence after only 1 h of incubation, and this decrease was greater than that observed for ZAC989 (Fig. 4D), despite ZAC307 having a 5-fold lower affinity for zinc than ZAC989. These data suggested that ZAC307, ZAC989 and TPEN were cell-permeable and bound intracellular zinc. In agreement with this, the extracellular chelator EDTA did not reduce the zinbo-5 fluorescence under the same conditions.

We investigated the propensity for resistance development to ZAC307 and ZAC989 by repeated exposure of *C. albicans* to ZACs in SDwoz media over a 36-day period. We observed no change in the MIC for the ZACs after repeated ZAC-exposure. In contrast, cells repeatedly exposed to fluconazole exhibited a significant increase in the MIC to fluconazole after 22 passages (Fig. 4E). Based on these results, it appeared that ZAC resistance was not easily induced in *C. albicans*.

ZACs efficiently inhibit the growth capacity of Aspergillus fumigatus under zinc-limiting conditions and their inhibitory effects are inactivated by zinc

In addition to potent antifungal effects on the five *Candida* species tested, ZAC307 and ZAC989 also potently inhibited the mold *Aspergillus fumigatus* and other *Aspergillus* species, as well a number of rare but very hard-to-treat members of the Mucorales order including *Rhizopus oryzae*, *Rhizopus microspores*, and *Mucor indicus*. The ZACs inhibited these molds and mucorales isolates in a range from 0.4 µg/mL to 5.4 µg/mL (Table 3). To assess the capacity of the ZACs to inhibit *A. fumigatus* growth in the presence of zinc, 1 mL aliquots of the sRPMI zinc-limiting medium, or this medium supplemented with 2, 5 or 50 µM zinc were inoculated with 10^5 conidia of a wild-type *A. fumigatus* strain (AF14), dispensed in 24-well culture plates and incubated in the presence of either ZAC307 or ZAC989 at a final concentration 21 µg/mL and 27 µg/mL (equivalent to 75 µM), respectively (Fig. 5A). Graphical representation and quantification of the fungal growth in 24-well culture plates in the presence of ZACs (Fig. 5A) revealed that the growth capacity of a wild-type *A. fumigatus* strain was reduced under zinc-limiting conditions but increased gradually when the growth medium was supplemented with increasing amounts of zinc, until fungal growth was fully restored when cultured in media supplemented with 50 µM Zn (i.e. under zinc replete conditions). Hence, the inhibitory effects of the ZACs against *A. fumigatus* were completely counteracted by simultaneous addition of zinc, similarly to our observations in *C. albicans* (Fig. 3C and 3D).

The zinc transporter ZrfC plays an important role in regulating fungal sensitivity to the ZACs

To ascertain whether ZAC307 and ZAC989 interfered with zinc uptake from the sRPMI zinc-limiting medium, we analyzed their effects on the growth capacity of the mutant strains AF48 (Δ*zrfA*Δ*zrfB*), AF721 (Δ*zrfA*Δ*zrfB*Δ*zrfC*), AF731 (Δ*zrfA*Δ*zrfB*Δ*zrfC* [*zrfC*]), which is an AF721 derivative strain that carries the *zrfC* gene reintroduced at the *pyrG* locus as described previously

(24), and AF54 (Δ*zrfC*) (Fig. 5B to Fig. 5E). The overall effect of the ZACs on the growth capacity of the AF48 strain was similar to that of the wild-type strain AF14 (compare Fig. 5A and 5B). In the absence of ZACs both strains exhibited a reduced the growth capacity from 100% to 70%, when cultured in media supplemented with 50 µM as compared to media supplemented with 2 µM zinc. This corresponded to a 1.4-fold reduction in growth capacity. However, in the presence of 2 µM zinc plus 75 µM ZAC307 the growth capacity of AF14 and AF48 was reduced respectively by 2.9 and 3.9-fold as compared to that in the presence of 50 µM zinc. Similarly, 2 µM zinc plus 75 µM ZAC989 reduced the growth capacity of AF14 and AF48 by 3.9 and 4.5-fold, respectively. The AF721 strain did not grow under zinc-limiting conditions, and hence the effect of these compounds could not be tested on this strain (Fig. 5C). The reintroduction of *zrfC* in a strain with a Δ*zrfA*Δ*zrfB*Δ*zrfC* genetic background restored the fungal growth capacity in the presence of the ZACs (Fig. 5D) at the same level as that of the wild-type and AF48 strains (Fig. 5A and 5B). Finally, in the presence of 2 µM zinc either with or without simultaneously exposure to ZAC307 or ZAC989 the growth capacity of the AF54 strain was reduced by an average of 24.6-fold as compared to its growth capacity in the presence of 50 µM zinc, (Fig. 5E), i.e. the ZACs were between 5 and 8-fold more efficient as inhibitors of the growth capacity of a Δ*zrfC* strain than of a wild-type or Δ*zrfA*Δ*zrfB* strain, which suggested that the effect of ZACs could be counteracted to a certain extent by the function of ZrfC.

ZAC307 and ZAC989 inhibit the transcription of genes regulated by ZafA under zinc-limiting conditions

The major regulator of the *A. fumigatus* zinc homeostatic response under zinc-limiting conditions is the transcription factor ZafA (11), which is a zinc-responsive factor that senses the intracellular concentration of zinc in a similar way to its orthologue Zap1 in the yeast *Saccharomyces cerevisiae*

(25). Thus, when the cytoplasmic zinc content is high enough, ZafA becomes saturated with Zn^{2+} ions and adopts a transcriptionally inactive conformation. In contrast, when the intracellular concentration drops below a certain threshold, ZafA begins to release Zn^{2+} ions and gradually adopts a transcriptionally active conformation, whereby it is able to induce the expression of *zrfA* and *zrfB* in acidic zinc-limiting media, and *zrfC* in alkaline zinc-limiting media (11, 24).

We employed qRT-PCR to assess whether exposure to ZAC307, ZAC989, EDTA or TPEN influenced the expression of several ZafA target genes and other genes not regulated directly by ZafA (as controls) (Table 4). The set of genes investigated was selected based on a genome-wide transcription analysis of *A. fumigatus* grown under zinc-limiting conditions that had been performed previously in our laboratory (Calera, JA; unpublished data), using the primers listed in Table 5. All selected ZafA target genes were induced by ZafA under zinc-limiting conditions with the exception of the putative zinc storage vacuole transporter *zrcA*, which was repressed by ZafA under zinc-limiting conditions (Calera JA; unpublished data). As expected, the relative expression levels of all ZafA target genes induced by ZafA under zinc-limiting conditions were dramatically reduced to almost undetectable levels upon the addition of Zn^{2+} (Fig. 6). In contrast, the expression level of the *zrcA* gene, which was repressed by ZafA, and most of the genes not regulated by ZafA increased under zinc-replete conditions to different extents, with the exception of *actA*, whose expression level remained similar to that observed before the zinc-shock. Interestingly, exposure to either ZAC307 or ZAC989 inhibited the expression of the ZafA target genes at similarly. We also observed reduced expression levels for most of the investigated genes that were not regulated by ZafA following ZAC307 exposure. In particular, the expression level of *pmaA*, which encodes the orthologue of the Pma1 H^+-ATPase from *S. cerevisiae*, and that of the *gdpA* and *tubB1* genes were reduced at levels similar to that of the ZafA target genes (Fig. 6). In contrast, treatment with ZAC989 did not have a noticeable effect on the expression levels of the genes not regulated by

ZafA, which remained similar to that observed under zinc-limiting conditions (Fig. 6). This finding suggested that although the overall outcome of the treatment with ZAC307 and ZAC989 on ZafA regulated genes was quite similar, the precise mode of action of ZAC307 on gene expression was different to that of ZAC989, which appeared to inhibit the ZafA regulated genes more specifically than ZAC307.

Finally, we anticipated that chelation of extracellular zinc upon addition of a relatively high concentration of EDTA to the culture media for a short period of time (2 h) would result in a transient hyperactivation of ZafA and concomitant upregulation of the most direct ZafA target genes, including those encoding zinc transporters. We expected to observe the same effect with TPEN treatment, although in this case chelation of intracellular zinc should exacerbate the zinc starvation status of the fungal cells, leading to a more extended hyperactivation of ZafA and higher expression of the ZafA target genes compared to that attained with EDTA after the same incubation period. The expression profile for the ZafA regulated genes observed in EDTA- or TPEN-treated cultures reflected precisely what we predicted (Fig. 6).

In summary, these results suggested that the antifungal effects of ZAC307 and ZAC989 were most likely mediated through a mechanism that ultimately results in the inhibition of the transcriptional activation activity of ZafA.

Cytotoxicity and off-target activity studies

ZAC307, ZAC989, EDTA and TPEN were evaluated for mammalian cytotoxicity in a standard hepatocyte cell proliferation assay, where the mammalian HepG2 cell line was exposed to the compounds for either 24 h or 72 h. After a 24 h exposure period to ZAC307 or ZAC989, the EC_{50} was >28 µg/mL, while after 72 h of exposure the EC_{50} was 13.2 µg/mL and 6.9 µg/mL, respectively (Table 6). With antifungal activity against yeast and the mucorales isolates in the 0.2 - 1.7 µg/mL

range, the compounds exhibited a reasonable selectivity index towards mammalian cells. However, the selectivity index between the *Aspergillus* species and mammalian cells was limited. The non-permeable chelator EDTA did not affect the proliferation of HepG2 cells, while the potent zinc chelator TPEN had an EC_{50} of 1.6 µg/mL after 24 h of exposure.

ZACs exhibit in vivo efficacy in a murine fungal kidney burden candidiasis model

ZAC989 and ZAC307 were investigated for *in vivo* efficacy in a fungal kidney burden model (Fig. 7, Table 7). In this model, BALB/c mice were infected intraperitoneally (IP) on day 0. Initially, administration of ZACs included a pre-treatment 24 h prior (day –1) to infection (day 0) by IP route. The mice were then treated with either ZAC for 4 days (day –1 to day 2) to maximize the likelihood of observing *in vivo* efficacy. The endpoint was mean log colony forming unit (CFU) in the kidneys of treated animals compared to untreated animals. Fluconazole was chosen as a comparator compound and dosed PO, and treatment with fluconazole resulted in a significant reduction in kidney burden of 2.78 log CFU/kidney (Fig. 7). The *in vivo* studies also revealed that IP dosing of ZAC989 at 60 mg/kg resulted in a statistically significant reduction of 1.71 log CFU/kidney, while ZAC307 administration at 60 mg/kg led to a significant reduction of 1.06 log CFU/kidney. ZAC307 yielded equal *in vivo* efficacy with or without pre-treatment (Fig. 7, Table 7). We observed no adverse effects following dosing of 60 mg/kg of ZAC307, but for ZAC989, we observed lethargy lasting for 5-15 minutes after dosing.

Discussion

During this study, we identified a new series of zinc attenuating compounds with broad-spectrum antifungal activity *in vitro* and *in vivo* activity in a candidiasis fungal kidney burden model. The compounds ZAC307 and ZAC989 possess a characteristic arrangement of an aromatic structure

with nitrogen bound in close proximity to a hydroxyl group. This structural arrangement led us to speculate whether ZAC307 and ZAC989 were metal chelators. To address this hypothesis, we synthesized ZAC623 as a control compound where the hydroxyl-group is replaced with an amino-group, and as expected this compound lacked metal-chelating and antifungal properties (Fig. 1, Table 1 and Fig. 3A). The metal chelating compounds EDTA and TPEN have previously been described as antifungal compounds (16, 17, 26), thus they were selected as comparators in this study.

Our findings indicate that ZAC307 and ZAC989 chelate both zinc and copper with zinc ions being most effective in reversing the growth inhibitory effects of the ZACs (Figure 3C and 3D). The ZACs has lower affinity for iron and negligible affinity for magnesium and calcium. The ZACs are less potent zinc chelators than the known zinc, copper and iron chelators TPEN and EDTA, but they inhibit fungal growth more effectively than EDTA (Fig. 3A and 3B). The inhibitory effects of the ZACs can be inactivated by the addition of excess zinc in both *Candida albicans* and *Aspergillus fumigatus*, which indicate that these compounds interfere either directly or indirectly with fungal zinc homeostasis.

The first challenge that any microorganism faces in the homeostatic response to zinc deficiency is to obtain zinc from the surrounding environment. The major components of the zinc uptake system in *A. fumigatus* that facilitates zinc uptake from zinc-limiting media are the ZIP plasma membrane transporters ZrfA, ZrfB and ZrfC. The ZrfA and ZrfB transporters operate mainly under acidic zinc-limiting conditions (27), although they also contribute to zinc uptake from alkaline zinc-limiting media along with ZrfC (3), which is expressed exclusively in alkaline media (24). Therefore, we reasoned that if the ZACs inhibited the intake of zinc mediated by these transporters, the growth capacity of a wild-type strain in the presence of ZACs should be reduced to the same level as that of fungal mutant strains lacking either the acidic (ZrfA and ZrfB) and/or the alkaline (ZrfC) zinc

transporter. The investigation of the growth capacity of a Δ*zrfC* mutant in the presence of the ZACs suggested that ZrfC plays an important role in overcoming ZAC inhibition, since deletion of *zrfC* increased the sensitivity of *A. fumigatus* to these compounds (AF14 vs. AF54, Fig. 5A and 5E). Hence, it could be possible that the actual effect of ZACs on the Δ*zrfA*Δ*zrfB* strain was masked to some extent by the ZrfC function. As expected, the AF721 strain lacking *zrfC* did not grow under zinc-limiting conditions, and effect of these compounds could therefore not be tested on this strain (Fig. 5C). However, we observed that ZAC989 noticeably inhibited the growth capacity of AF721 in the presence of 50 µM zinc. Thus, it is plausible that ZAC989 interfered with a zinc homeostatic process other than zinc uptake. Furthermore, the higher growth capacity of the Δ*zrfC* strain in the absence of ZACs compared to that of the wild-type, AF48 or AF731 strain, suggested that the lack of *zrfC* in AF54 may have been compensated for by the overexpression of *zrfA* and *zrfB*, as reported previously (3). On the other hand, the stronger growth inhibition of the growth capacity of the AF54 strain in the presence of ZAC307 and ZAC989 compared to that of the wild-type, AF48 or AF731 strain suggested that the expression levels of the *zrfA* and *zrfB* genes in AF54 were insufficient to counteract the effects of ZAC307 and ZAC989. Taken together, these results suggest that both ZAC307 and ZAC989 interfered negatively with the expression of the genes encoding zinc transporters rather than with their zinc uptake function. Indeed, gene expression analysis by RT-qPCR suggested that the antifungal effects of ZAC307 and ZAC989 were mediated through a mechanism that ultimately results in inhibition of the transcriptional activation activity of ZafA. In addition, and since ZafA activity was inactivated by zinc under physiological conditions, the effects of ZAC307 and ZAC989 on the expression of ZafA-regulated genes could be exerted either directly, upon their binding to ZafA, or indirectly, by increasing the cytosolic concentration of Zn^{2+} ions that would bind to and inactivate ZafA. Although direct binding of ZAC307 or ZAC989 to ZafA was an attractive possibility, we consider it more likely that the ZACs triggered a transient

rise in the cytosolic concentration of Zn^{2+} ions by favoring their releasing from cytosolic zinc ligands and/or zinc storage compartments (e.g. the vacuole). In the data presented in Fig. 4D we observed that the ZACs promote a decrease in the available zinc levels within the internal membrane system including the ER in *C. albicans*. This decrease can be explained either by a direct competition between zinbo-5 and ZACs within these compartments, or because the ZACs promote the release of zinc from the ER into the cytosol. The latter scenario could induce a higher concentration of zinc in the cytosol, and if the same situation occurs in *A. fumigatus* this could explain the decrease in transcription of the ZafA induced genes similarly to when zinc is added extracellularly. Moreover, since most intracellular eukaryotic zinc proteins bind zinc with a higher affinity than ZACs (K_d values for most zinc binding proteins are between 0.1 and 1.0 pM) (28), it is more likely that these compounds interfere with the regulation of zinc homeostasis by promoting the release of Zn^{2+} ions from intracellular storage compartments. Nevertheless, since acidification of cytoplasm can also promote zinc release from cytoplasmic zinc ligands (29), it could also be possible that the ZACs disturbed the activity of proteins involved in maintaining the pH homeostasis of the cytoplasm. In this regard, we observed that the expression level of *pmaA* was higher under zinc-replete than under zinc-limiting conditions. This finding suggests a putative interplay between the function of PmaA and the Zn^{2+} transport capacity of the fungal zinc transporters, provided that the expression level of the *pmaA* gene correlated with the H^+-ATPase (PmaA) activity. It is known that the accumulation of zinc into the vacuole by CDF transporters (e.g. ZrcA) is mediated through a Zn^{2+}/H^+ antiporter mechanism and it relies on the proton gradient generated by the V-ATPase (30). In contrast, and although it is not completely known how ZIP proteins transport zinc across the plasma membrane, it seems that it is not dependent on the proton gradient generated by the plasma membrane H^+-ATPase but pH-dependent, such that intracellular acidification increases zinc transport whereas extracellular acidification decreases zinc transport

(31–33). In this regard, it is plausible that in the alkaline zinc-limiting conditions provided by the sRPMI medium, a low PmaA activity would increase intracellular acidification to favor zinc uptake by ZIP transporters located in the plasma membrane. In contrast, a high PmaA activity under zinc-replete conditions would reduce intracellular acidification and increase extracellular acidification (e.g. to counteract the Zn^{2+}-induced dissipation of the electrochemical gradient that is essential for fungal survival). The same reasoning could be applied to zinc transport by the ZrfF ZIP transporter located in the vacuolar membrane, such that the intravacuolar pH, which is kept lower than the cytosolic pH under normal conditions via V-ATPase activity, would favor the exit of Zn^{2+} ions into the cytosol. However, the unexpected finding that ZAC307 reduces *pmaA* expression suggested that it might interfere with the putative mechanism that links the regulation of zinc homeostasis with the function of PmaA.

The ZACs display broad-spectrum fungistatic activity and exhibit a low propensity for acquired resistance development, compared to fluconazole. Additionally, they are superior antifungal agents than the non-permeable chelator EDTA, and our qRT-PCR data suggest that the ZACs affect fungal zinc homeostasis differently to the very potent chelator TPEN. Therefore, the ZACs act distinctly from either EDTA or TPEN, both of which have previously been investigated as antifungal agents. EDTA has been evaluated as a combination treatment together with amphotericin B lipid complex (ABLC) in an invasive pulmonary aspergillosis model in immunosuppressed rats. The combination of EDTA with ABLC led to improved survival times and a lower tissue burden of *A. fumigatus* than either agent alone (26). Furthermore, TPEN has been shown to significantly increase survival after 7 days compared to vehicle treatment in a murine model of invasive pulmonary aspergillosis (16). Moreover, administration of either of the two zinc-chelating agents phenanthroline or TPEN has been shown to lead to significant improvements in survival with concomitant reduction in fungal burden in immunosuppressed mice intranasally infected with *A. fumigatus*. Finally, it was shown

405 that TPEN given in combination with caspofungin significantly increased survival times in murine
406 models of invasive aspergillosis compared to either drug alone (17).
407 There is an unmet need for novel antifungal agents with broad-spectrum antifungal activity and low
408 potential for resistance development for the treatment of invasive fungal infections. With potent
409 antifungal activity both *in vitro* and *in vivo*, the ZACs fulfil these criteria and their advancement in a
410 drug development program is therefore warranted. Interestingly, the ZACs and EDTA did not
411 inhibit mammalian cell proliferation considerably within the first 24 h of exposure (EC_{50} > 28
412 µg/mL) in contrast to TPEN (EC_{50} = 1.6 µg/mL), and even after 72 h of ZAC exposure we observed
413 a >12-fold selectivity index in growth inhibition between *C. albicans* and HepG2 cells, but the
414 index between *A. fumigatus* and HepG2 cells was limited. However, it should be taken into account
415 that metal ions are crucial in every cellular system, including the host. Therefore, any intervention
416 aiming to treat an infection through ion sequestration must deal with the delicate balance between
417 positive and negative effects both in the pathogen and the host. The therapeutic safety window as
418 well as the question about whether the ZACs can induce zinc deficiency in the host still need to be
419 addressed. In summary, interfering with fungal zinc-dependent processes represents a promising
420 new approach to antifungal therapy and this series of zinc attenuating compounds represents a
421 potentially new class of antifungal agents.
422
423 **Materials and methods**
424 **Synthesis of ZAC307, ZAC989, and ZAC623**
425 ZAC307: (2-[6-(dimethylamino)pyrimidin-4-yl]-5-phenyl-pyrazol-3-ol): **a**: i) *N*-Methylmethan-
426 amine, TEA, 2-propanol, 0 °C, 2h, evaporate, ii) Hydrazine hydrate, reflux, 2h, column
427 chromatography, Yield 65%; **b**, Ethyl 3-oxo-3-phenyl-propanoate2-propanol, reflux, 1h, yield:

69%, 1H NMR (400 MHz; DMSO-d_6, d): 13.2 (1H, bs), 8.49 (1H, d), 7.89 (2H, bd), 7.43 (3H, m), 6.92 (1H, bs), 6.13 (H, s) and 3.17 (6H, s).

ZAC989: (3-[(3*S*)-1-[6-(5-hydroxy-3-methyl-pyrazol-1-yl)pyrimidin-4-yl]pyrrolidin-3-yl]oxy-pyridine-4-carbonitrile): **a**, NaH, abs. *tert*-butyl (3S)-3-hydroxypyrrolidine-1-carboxylate, THF, 0 °C, 3h, NH_4Cl, 82%; **b**, Diethylether, conc. HCl, 0 °C , quant.; **c**, Load onto SCX in methanol, elute with 1M NH_3 in MeOH, 95%; **d**, (2-(6-chloropyrimidin-4-yl)-5-methyl-pyrazol-3-ol): (6-chloropyrimidin-4-yl)hydrazine and methyl 3-oxobutanoate 2-propanol, reflux 90 min, 14%; **e**, 2-(6-chloropyrimidin-4-yl)-5-methyl-pyrazol-3-ol and product from **c**, NMP, DIPEA, 30 min at 100 °C, 89%, 1H NMR (400 MHz; DMSO-d_6, δ): 8.84 (s, 1H), 8.46 (d, 1H), 8.42(d, 1H), 7.77 (dd, 1H), 7.08 (bs, 1H), 5.59 (bs, 1H), 5.24 (bs, 1H), 3.95 (dd, 1H), 3.81 (bs, 2H), 3.68 (dq, 1H), 2.43-2.50 (m, 1H), 2.35-2.40 (m, 1H), 2.19 (s, 3H).

ZAC623: (3-[(3*S*)-1-[6-(5-amino-3-methyl-pyrazol-1-yl)pyrimidin-4-yl]pyrrolidin-3-yl]oxypyridine-4-carbonitrile): **a**, *tert*-Butyl-*N*-aminocarbamate, DIPEA, THF, rt → reflux, 98%; **b**, Pyrrolidine from ZAC989-c, DIPEA, NMP, 120 ^{o}C , 1h, 71%; **c**, i) TFA, DCM, rt, 30 min, ii) Load onto SCX in methanol, elute with 0.5M NH_3 in MeOH, quant.; **d**, *Z*-3-Amino-but-2-enenitrile, AcOH, EtOH, 80 °C 4h, 85%. 1H NMR (500 MHz; DMSO-d_6, δ): 8.80 (s, 1H), 8.36 (d, 1H), 8.30(d, 1H), 7.78 (dd, 1H), 6.84 (s, 1H), 6.65 (bs, 1H), 5.54 (bs, 1H), 5.21 (s, 1H), 3.81 (bs, 2H), 3.61 (bs, 2H), 2.25-2.46 (bs, 2H), 2.07 (s, 3H).

Fungal isolates and growth conditions

Fungal isolates used in this study were purchased from either ATCC, DSMZ (Germany) or the Danish National Serum Institute (SSI), with the exception of *C. glabrata* strain Cg003, which was a kind gift from Julius Subik, Comenius University in Bratislava, Slovak Republic. *C. glabrata* Cg003 is clinical isolate 3 previously used by Berila and Subik (2010) and was characterized to be

resistant to fluconazole and itraconazole via overexpression of the multidrug resistance efflux pumps Cdr1p and Cdr2p (34). *Aspergillus terreus* isolate At070 was a kind gift from Herning Hospital, Denmark. The *Aspergillus fumigatus* strains AF14, AF54, AF48, AF721 and AF731 have previously been described previously (3, 24, 27).

Candida albicans (SC5314), *C. glabrata* (ATCC-90030), *C. glabrata* (Cg003), *C. krusei* (ATCC-6258), *C. parapsilosis* (ATCC-22019) and *C. tropicalis* (Ct016) were grown in Sabouraud broth (40 g/L d-glucose, 10 g/L peptone, pH 5.6) or YPD (10 g/L yeast extract, 20 g/L Bacto-peptone, 20 g/L glucose) liquid media to mid-log phase, aliquoted into a final concentration of 20% (v/v) glycerol and maintained as frozen stocks at –80 °C. Freeze stocks of the mold isolates (*A. fumigatus* (ATCC-13073), *A. flavus* (ATCC-15547), *A. terreus* (At070), *Rhizopus oryzae* (ATCC-34965), *R. microsporus* (ATCC-66276) and *Mucor indicus* (ATCC-MYA-4678)) were prepared by harvesting spores from 7-day old potato glucose agar plates in PBS containing 0.1% Tween-80, and aliquoting these spores in the presence of glycerol at a final concentration of 20% (v/v).

SD media without zinc (SDwoz: 1.71 g/L YNB-$ZnSO_4$ (1541, Sunrise Science), 2% glucose, 5 g/L ammonium sulphate) was prepared in a glass beaker washed with 0.37% HCl and rinsed with water. The pH was adjusted to 7.0 with NaOH and the media was sterile by filtration.

Dissociation constant determination

The dissociation constant (K_d) of zinc to zinc-attenuating compounds was determined at room temperature using FluoZin-3 (F24194, ThermoFisher Scientific), which has a K_d, Fluozin-3:Zn^{2+} = 15 nM (35). Testing buffer consisted of PBS pH 7.4 with 200 nM $ZnCl_2$ and 500 nM FluoZin-3. In a microtiter plate, 98 µL testing buffer was mixed with 2 µL compound at a range of concentrations to determine the IC_{50}. Testing plates were incubated for 2 min before reading at Ex = 485 and Em =

516 with a Fluoroskan Ascent Microplate Fluorometer, ThermoScientific. The K_ds were calculated using the equation: K_d (compound:Zn^{2+}) = IC50 / (1 + [Fluozin-3] / K_d,Fluozin-3:Zn^{2+}) (36).

Potentiometric titration

Potentiometric measurements were carried out in DMSO/water (70:30 v/v) at 25 °C as described previously (22). Titrations were performed with a pH meter (Denver Instrument) utilizing a glass electrode with AgCl reference filled with 3.0 M KCl. The electrode was equilibrated in DMSO/water (70:30 v/v) for at least 1 h before use. All experiments were performed at constant ionic strength (0.1 M $NaClO_4$). Three millilitres of a solution containing 1 mM compound was titrated with 0.3 M NaOH by manual additions in 1-5 µL increments under magnetic stirring. The metal-ligand binding constants were obtained from titrations of the metal complex solutions prepared in a 1:2 metal-to-ligand ratio. The titration data were refined by the nonlinear least squares refinement program Hyperquad2013 (37) to determine the deprotonation and stability constants.

Antifungal susceptibility testing

Antifungal susceptibility testing was carried out as described previously (38, 39) with a few modifications. Briefly, for each yeast or mold growth inhibition assay, frozen stocks of yeast cells or spores were diluted to a final concentration of 0.5-2.5 × 10^5 CFU/ml in sterile water. ZAC989, ZAC307 and ZAC623 were dissolved in DMSO to 10 mM stocks from which half-log serial dilutions were prepared from this. Growth assays were subsequently performed by pipetting 3 µL compound dissolved in DMSO (giving a final concentration of 1.5% DMSO), 100 µL cell/spore suspension and 97 µL 2× RPMI-media (20.8 g/L RPMI-1640 media, 69.06 g/L MOPS, 36 g/L glucose) into a microtiter plate that was incubating for 24 h (yeasts) or 48-72 h (molds) at 34 ºC. Fungal growth was determined spectrophotometrically by optical density reading of each well at a

wavelength of 492 nm on a Victor X5 (Perkin-Elmer) plate reader. The minimum inhibitory concentration (MIC) was defined as the lowest compound concentration that resulted in at least 50% growth inhibition for yeast, which corresponded to a prominent decrease in visible growth. For the molds the MIC was defined as the lowest concentration of the compound that resulted in no visible growth. Standard errors between repeated experiments were generally below 5%. The growth effect of exogenous addition of various divalent metals was evaluated by performing the antifungal susceptibility assay in the presence of 5 µM of ZAC989 or ZAC307 and with increasing concentrations (0.003 - 50 µM) of $ZnSO_4$, $CuSO_4$, $(NH_4)_2Fe(SO_4)_2$, $MgCl_2$, and $CaCl_2$. The MFC was the minimum concentration that resulted in no colony forming units and was determined after MIC determination by plating 5 µL of the mixture from wells with no visible growth onto YPD agar plates followed by 24 h incubation at 30 °C.

Growth capacity experiments with the *A. fumigatus* strains AF14, AF54, AF48, AF732 and AF731 were performed in 24-well flat-bottomed tissue culture plates (35-3047, Falcon). A stock solution of 10 mM TPEN (P4413, Sigma) was prepared in pure ethanol. For these experiments, 5 mM stock solutions of ZAC307 and ZAC989 were prepared by dissolving each compound in 80% (v/v) ethanol. A 0.5 M stock solution of $Na_2EDTA\text{-}2H_2O$ (1.08421.1000, Merck) was prepared in sterile water. A 1× stock solution (10.4 g/L) of the RPMI-1641 medium (R8755, Sigma) supplemented with 10 µM $FeSO_4\text{-}7H_2O$, 1 µM $CuSO_4\text{-}5\ H_2O$ and 1 µM $MnCl_2\text{-}H_2O$ (sRPMI) was prepared under aseptic conditions and used as standard culture medium. In each well, 1 mL of culture medium containing sRPMI medium, Tween-20, ethanol (or the specified compound dissolved in 80% ethanol) and 10^5 conidia was dispensed, to achieve a final concentration of 0.7×, 0.05% (v/v), 1.2% (v/v) and 10^5 conidia/mL, respectively. Plates were incubated for 44 h at 37 ºC in a humid atmosphere. To quantitate mycelial growth, each plate was scanned in the Agfa SnapScan 1236s scanner, and the intensity of the wells was quantified using the open source image processing

program Image J2. The data were represented and analyzed with the Prism Software 7.0.

Time-kill assay

C. albicans SC5314 cells (10^5 CFU/mL) were incubated in 10 mL RPMI media at 30°C with gentle agitation (150 rpm) in the presence of EDTA (15 µM), TPEN (10 µM), ZAC989 (10 µM) or AMB (0.5 µM). At the indicated time points (0, 3, 5.5 and 24 h), a 100-µL aliquot was removed for each test condition, serially diluted (10-fold) in saline (0.9% NaCl), and 30 µL of each dilution was plated on YPD agar plates. The colony count on each YPD plate was determined after incubation at 30 °C for 48 h (40). *C. albicans* cells treated with DMSO (1%, v/v) served as a control.

Resistance study

The propensity for resistance development was investigated as also described previously (41), but with the following modifications. *C. albicans* was repeatedly exposed to either ZAC989 or ZAC307 in 1 mL cultures in SDwoz media with a starting inoculum of OD_{600}=0.007. A compound concentration that resulted in ~90% growth inhibition was selected for these experiments; (3.6 µg/mL for ZAC989, 2.8 µg/mL and 5.6 µg/mL for ZAC307, 0.5 µg/mL and 1.0 µg/mL for fluconazole). Over a 36-day period, culture aliquots of 100 µL were periodically (every 1-2 days) transferred (passaged) to new culture tubes with 900 µL fresh media and fresh compound. The cells were incubated at 30 °C, with gentle agitation (150 rpm), and the OD_{600} of cultures was monitored throughout the entire period to ensure that the number of cells exposed to compounds was comparable across treatments for each passage. Cells were passaged a total of 22 times, and cultures were periodically tested for antifungal susceptibility following the protocol for antifungal susceptibility testing, as described above.

Zinbo-5 assay

C. albicans BWP17 was grown overnight in YPD media at 30 °C and 150 rpm. The cells were pelleted, washed in PBS buffer (D8537, Sigma) 3 times and re-suspended to an OD_{600} of 2.0. Two microliters of compound in DMSO was mixed with 100 µL cell suspension and incubated statically for 1, 8 or 24 h at 30 °C in a 96-well black plate. Thirty minutes before the end of the incubation period, 100 µL of 10 µM zinbo-5 (sc-222425, Santa Cruz Biotechnology) in PBS buffer was added. The affinity constant of this probe for zinc is 2.2 nM (23). The plate was then read on a plate reader (FLUOstar Optima, BMG Lab technologies) with excitation at 355 nm and emission at 485 nm. Decrease in zinbo-5 fluorescence was calculated relative to the untreated DMSO-control.

RNA isolation from *Aspergillus fumigatus*

1.5×10^6 conidia of the wild-type strain (AF14) were inoculated into 20 mL of 0.7× sRPMI, 0.05% Tween-20 and 1.2 % ethanol dispensed into 100-mL culture flasks pre-treated by a over night wash in 2 mM EDTA pH 8.0 to minimize the presence of metal traces followed by an thoroughly washing with ultrapure Milli-Q water. Then flasks were subsequently sterilized in an oven at 180 ºC. The cultures were incubated for 20 h at 37 ºC and 200 rpm before the following was added: (1) pure ethanol to a final concentration of 1.2 % (v/v) (as a reference for the transcription profiles of all genes under zinc-limiting conditions); (2) 1.2 % ethanol plus a solution of $ZnSO_4$ to a final concentration 20 µM zinc (as a reference for the transcription profiles of all genes under zinc-replete conditions following the zinc-shift); (3) 1.2 % ethanol plus a solution of EDTA to a final concentration of 500 µM; (4) 1.2 % ethanol plus a solution of TPEN to a final concentration of 10.6 µg/mL, and (5) a 5 mM solution of each test compound (ZAC307 or ZAC989) dissolved in 80 % ethanol to a final concentration of 75 µM and 1.2 % ethanol, (which corresponds to 21 µg/mL and 27 µg/mL, respectively). After compound addition, cultures were incubated for 2 h at 37 ºC and 200

rpm and mycelia were harvested by filtration through filter paper, washed twice with sterile water and snap-frozen in liquid nitrogen. After grinding the mycelia in the presence of liquid nitrogen, total RNA was extracted using the RNeasy Plant Mini Kit (74904, QIAGEN) according to the manufacturer's instructions. RNA was eluted in 50 µL of RNase-free water. RNA integrity was verified on 0.8 % agarose gels stained with ethidium bromide. RNA was stored at –80 ºC until use.

RT-qPCR

Total RNA concentration and quality was determined by UV spectrometry (Nanodrop ND1000 spectrophotometer, Thermo Fisher Scientific) and all samples were brought to a final concentration of 150 ng/µL. Total RNA 1.5 µg was treated with RQ1 DNase I (M610, Promega) and subsequently assessed by conventional PCR for the complete absence of gDNA. Subsequently, 1 µg of DNase-treated RNA was reversed transcribed using the SuperScript II Reverse Transcriptase (18064-014, Invitrogen, Thermo Fisher Scientific) using random hexamers (11034731001, Roche Diagnostics) as primers. Prior to qPCR reactions, cDNA samples were diluted 1:3 in water, except for reactions against the 18S rRNA that were diluted 1:1200 in water. qPCR reactions were performed on a BioRad CFX96 instrument. A typical qPCR reaction mixture (10 µL) contained 13.5 ng cDNA (32 pg when the qPCR was for 18S rRNA), a specific pair of primers (150 nM final concentration), and the SYBR Premix ExTaq (RR420A, Takara). Primers used for qPCR are listed in Table 3. For all qPCR reactions, 40 cycles were performed using the following cycling conditions: denaturation at 95 ºC for 10 seconds, annealing at 59 ºC for 20 seconds and extension at 72 ºC for 20 seconds. The relative expression ratio (rER) was calculated using the $2^{-\Delta\Delta Ct}$ method (42) using the expression level of the 18S rRNA as an internal reference.

Human hepatocyte (HepG2) proliferation assay

In each well of a 96-well tissue culture plate (GR-655180, Grenier), 10,000 human hepatocyte (HepG2) cells (85011430, Sigma) were plated in 200 µL growth media (EMEM (M2279, Sigma), supplemented with 2 mM L-Glutamine (03-020-1B, Biological Industries), 1 % non-essential amino acids (XC-E1154/100, Biosera), and 10 % fetal bovine serum (BI-04-007-1A, Biological Industries)), and plates were incubated overnight at 37 °C and 5 % CO_2. The following day, fresh growth media plus 2 µL compound in DMSO was added. The plate was incubated for a further 24 h or 72 h at 37 °C and 5 % CO_2. The media was then replaced with 100 µL freshly prepared XTT sodium salt solution (0.5 mg/mL XTT; X4251, Sigma) in RPMI-1640 (R7509, Sigma-Aldrich) with 3.83 µg/mL phenazine methosulfate (P9625, Sigma-Aldrich) and incubated 2 - 3 h at 37 °C and 5 % CO_2 (43). The color reaction was measured on Victor X5 plate reader (Perkin-Elmer) at OD_{450} and the half maximal effective concentration (EC_{50}) was calculated. Tamoxifen (85256, Sigma) was used as a positive control compound.

In vivo fungal kidney burden candidiasis model

A murine model of systemic candidiasis was established according to a previously described method (44). BALB/c mice were infected with a 0.1 mL inoculum (1-5 × 10^5 CFU) of *Candida albicans* SC5314 cells by intravenous route on day 0. Compounds were tested at doses of 60 mg/kg. Administration of compound was initiated 24 h prior (day -1) to infection (day 0) by intraperitoneal route, dosing twice a day for 4 days (day -1 to day 2). ZAC307 was also evaluated with administration of the compounds given after the infection at day 0 (no pre-treatment) and with following dosing twice a day for 3 days (day 0 to 2). Fluconazole was used as a comparator drug. Six mice were used for each group and the untreated control group was exposed to the vehicle alone. ZAC989 and ZAC307 were formulated by taking 60 mg of compound and adding this to 2 mL and 4 mL of 0.1 N NaOH, respectively. After mixing and sonicating the resulting solutions, 4

mL of purified water was added. The pH was adjusted to pH 9.0 with 0.1N HCl solution followed by the addition of 90 mg of NaCl. The solutions were then diluted to 10 mL and filtered through 0.22 µm PVDF filter. Sample collection and processing was performed as follows: 12 h post last dose, all treated and untreated animals were sacrificed by cervical dislocation and kidneys were collected in 3 mL of sterile normal saline. The samples were homogenized, serially diluted and plated on SDA. SDA plates were incubated for 24 - 48 h at 35 °C, and CFUs were enumerated and reported as log CFU/kidney. Endpoint: Mean log CFU of fungi in kidneys of treated animals compared to that of untreated animals. The study was conducted in conformance with an application submitted to CPCSEA, New Delhi (Committee for the Purpose of Control and Supervision of Experiments on Animals) after approval from the Institutional Animal Ethics Committee (IAEC).

Acknowledgements

We are grateful to Sandra Gordon and Anne Louise Mortensen for assistance with experimental procedures and to John Bondo Hansen and Lars Dalgaard for discussions about fungal *in vivo* studies. L.K. was supported by Innovation Fund Denmark, DK (4019-00019B). K.O.C., J.D.C., L.K., W.D.B., and A.L.W are or were employed of Pcovery. L.M. is employed by the Consejo Superior de Investigaciones Científicas (CSIC) and J.A.C. is employed by the Universidad de Salamanca (Spain). Pcovery has filed a patent relating to the compounds described in this publication, but do not have any product in development or marketed product related to this publication. There are no other competing interests to declare. Pcovery ApS received funding from Wellcome Trust Research Councils, UK (100480/Z/12), Novo Seeds, DK and Boehringer Ingelheim Venture Fund, D. J.A.C. thanks the Spanish Ministry of Economy and Competitiveness

642 for financial support through grant SAF2013-48382-R. The funders had no role in study design,
643 data collection and interpretation, or the decision to submit the work for publication.

644

645 **Author contributions**

646 A.L.W. and W.D.B. initiated the project. S.C., T.D.P., and W.D.B. designed the compounds and
647 chemical synthesis. L.K., K.O.C., J.D.C., and A.L.W performed the biological experiments with
648 *Candida albicans*. L.M. and J.A.C. designed and performed the biological studies with *Aspergillus*
649 *fumigatus* mutants and the RT-qPCR studies. All authors participated in data analysis, and K.O.C.,
650 J.A.C., and A.L.W. wrote the paper with comments from all authors.

651 **References**

652 1. Hood MI, Skaar EP. 2012. Nutritional immunity: transition metals at the pathogen-host
653 interface. Nat Rev Microbiol 10:525–537.

654 2. Soares MP, Weiss G. 2015. The Iron age of host-microbe interactions. EMBO Rep 16:1482–
655 1500.

656 3. Amich J, Vicentefranqueira R, Mellado E, Ruiz-Carmuega A, Leal F, Calera JA. 2014. The
657 ZrfC alkaline zinc transporter is required for Aspergillus fumigatus virulence and its growth
658 in the presence of the Zn/Mn-chelating protein calprotectin. Cell Microbiol 16:548–564.

659 4. Urban CF, Ermert D, Schmid M, Abu-Abed U, Goosmann C, Nacken W, Brinkmann V,
660 Jungblut PR, Zychlinsky A. 2009. Neutrophil extracellular traps contain calprotectin, a
661 cytosolic protein complex involved in host defense against Candida albicans. PLoS Pathog
662 5:e1000639.

663 5. Bianchi M, Niemiec MJ, Siler U, Urban CF, Reichenbach J. 2011. Restoration of anti-
664 Aspergillus defense by neutrophil extracellular traps in human chronic granulomatous
665 disease after gene therapy is calprotectin-dependent. J Allergy Clin Immunol 127:1243–
666 1252.

667 6. Crawford A, Wilson D. 2015. Essential metals at the host-pathogen interface: nutritional
668 immunity and micronutrient assimilation by human fungal pathogens. FEMS Yeast Res
669 15:pii: fov071.

670 7. Caza M, Kronstad JW. 2013. Shared and distinct mechanisms of iron acquisition by bacterial
671 and fungal pathogens of humans. Front Cell Infect Microbiol 3:80.

672 8. Haas H. 2012. Iron - a key nexus in the virulence of Aspergillus fumigatus. Front Microbiol
673 3:28.

674 9. Corbin BD, Seeley EH, Raab A, Feldmann J, Miller MR, Torres VJ, Anderson KL, Dattilo
675 BM, Dunman PM, Gerads R, Caprioli RM, Nacken W, Chazin WJ, Skaar EP. 2008. Metal
676 chelation and inhibition of bacterial growth in tissue abscesses. Science 319:962–965.

677 10. Lulloff SJ, Hahn BL, Sohnle PG. 2004. Fungal susceptibility to zinc deprivation. J Lab Clin
678 Med 144:208–214.

679 11. Moreno MA, Amich J, Vicentefranqueira R, Leal F, Calera JA. 2007. Culture conditions for
680 zinc- and pH-regulated gene expression studies in Aspergillus fumigatus. Int Microbiol
681 10:187–192.

682 12. Staats CC, Kmetzsch L, Schrank A, Vainstein MH, Zamboni DS, De U, Paulo S, Mitchell A.
683 2013. Fungal zinc metabolism and its connections to virulence. Front Cell Infect Microbiol
684 3:65.

685 13. Broxton CN, Culotta VC. 2016. SOD Enzymes and Microbial Pathogens: Surviving the
686 Oxidative Storm of Infection. PLoS Pathog 12:e1005295.

687 14. Clark HL, Jhingran A, Sun Y, Vareechon C, de Jesus Carrion S, Skaar EP, Chazin WJ,
688 Calera JA, Hohl TM, Pearlman E. 2016. Zinc and Manganese Chelation by Neutrophil
689 S100A8/A9 (Calprotectin) Limits Extracellular Aspergillus fumigatus Hyphal Growth and
690 Corneal Infection. J Immunol 196:336–344.

691 15. Santos ALS, Sodre CL, Valle R., Silva BA, Abi-chacra EA, V. Silva L, Souza-Goncalves
692 AL, Sangenito LS, Goncalves DS, Souza LOP, Palmeira VF, d'Avila-Levy CM, Kneipp LF,
693 Kellett A, McCann M, Branquinha MH. 2012. Antimicrobial Action of Chelating Agents:
694 Repercussions on the Microorganism Development, Virulence and Pathogenesis. Curr Med
695 Chem 19:2715–2737.

696 16. Hein KZ, Takahashi H, Tsumori T, Yasui Y, Nanjoh Y, Toga T. 2015. Disulphide-reduced

psoriasin is a human apoptosis- inducing broad-spectrum fungicide. Proc Natl Acad Sci U S A 5:2–7.

17. Laskaris P, Atrouni A, Calera JA, D'Enfert C, Munier-lehmann H, Cavaillon J-M, Latgé J-P, Ibrahim-Granet O. 2016. Administration of zinc chelators improves survival of mice infected with Aspergillus fumigatus both in monotherapy and in combination with caspofungin. Antimicrob Agents Chemother 60:5631–5639.

18. Vicentefranqueira R, Amich J, Laskaris P, Ibrahim-Granet O, Latgé JP, Toledo H, Leal F, Calera JA. 2015. Targeting zinc homeostasis to combat Aspergillus fumigatus infections. Front Microbiol 6:1–7.

19. Kjellerup L, Gordon S, Cohrt KO, Brown WD, Fuglsang AT, Winther A-ML. 2017. Identification of antifungal H+-ATPase inhibitors with effect on the plasma membrane potential. Antimicrob Agents Chemother 61:e00032-17.

20. Clausen JD, Kjellerup L, Cohrt KO, Hansen JB, Dalby-Brown W, Winther A-ML. 2017. Elucidation of antimicrobial activity and mechanism of action by N- substituted carbazole derivatives. Bioorg Med Chem Lett 27:4564–4570.

21. Fahrni CJ, O'Halloran T V. 1999. Aqueous coordination chemistry of quinoline-based fluorescence probes for the biological chemistry of zinc. J Am Chem Soc 121:11448–11458.

22. Sanvar Nasir M, Fahrni CJ, Suhy DA, Kolodsick KJ, Singer CP, O'Halloran T V. 1999. The chemical cell biology of zinc: Structure and intracellular fluorescence of a zinc-quinolinesulfonamide complex. J Biol Inorg Chem 4:775–783.

23. Taki M, Wolford JL, O'Halloran T V. 2004. Emission Ratiometric Imaging of Intracellular Zinc: Design of a Benzoxazole Fluorescent Sensor and Its Application in Two-Photon Microscopy. J Am Chem Soc 126:712–713.

720 24. Amich J, Vicentefranqueira R, Leal F, Calera JA. 2010. Aspergillus fumigatus survival in
721 alkaline and extreme zinc-limiting environments relies on the induction of a zinc homeostasis
722 system encoded by the zrfC and aspf2 genes. Eukaryot Cell 9:424–37.

723 25. Wilson S, Bird AJ. 2016. Zinc sensing and regulation in yeast model systems. Arch Biochem
724 Biophys 611:30–36.

725 26. Hachem R, Bahna P, Hanna H, Stephens LC, Hachem R, Bahna P, Hanna H, Stephens LC,
726 Raad I. 2006. EDTA as an Adjunct Antifungal Agent for Invasive Pulmonary Aspergillosis
727 in a Rodent Model EDTA as an Adjunct Antifungal Agent for Invasive Pulmonary
728 Aspergillosis in a Rodent Model. Antimicrob Agents Chemother 50:1823–27.

729 27. Vicentefranqueira R, Moreno MA, Leal F, Calera JA. 2005. The zrfA and zrfB genes of
730 Aspergillus fumigatus encode the zinc transporter proteins of a zinc uptake system induced in
731 an acid, zinc-depleted environment. Eukaryot Cell 4:837–848.

732 28. Maret W, Li Y. 2009. Coordination dynamics of zinc in proteins. Chem Rev 109:4682–4707.

733 29. Kiedrowski L. 2014. Proton-dependent zinc release from intracellular ligands. J Neurochem
734 130:87–96.

735 30. MacDiarmid CW, Milanick MA, Eide DJ. 2002. Biochemical properties of vacuolar zinc
736 transport systems of saccharomyces cerevisiae. J Biol Chem 277:39187–39194.

737 31. Colvin RA. 2002. pH dependence and compartmentalization of zinc transported across
738 plasma membrane of rat cortical neurons. Am J Physiol Cell Physiol 282:C317–C329.

739 32. Lin W, Chai J, Love J, Fu D. 2010. Selective electrodiffusion of zinc ions in a Zrt-, Irt-like
740 protein, ZIPB. J Biol Chem 285:39013–39020.

741 33. Pedas P, Husted S. 2009. Zinc transport mediated by barley ZIP proteins are induced by low
742 pH. Plant Signal Behav 4:842–845.

743 34. Berila N, Subik J. 2010. Molecular analysis of Candida glabrata clinical isolates.
744 Mycopathologia 170:99–105.

745 35. Gee KR, Zhou ZL, Qian WJ, Kennedy R. 2002. Detection and imaging of zinc secretion
746 from pancreatic beta-cells using a new fluorescent zinc indicator. J Am Chem Soc 124:776–
747 778.

748 36. Cheng Y, Prusoff WH. 1973. Relationship between the inhibition constant (KI) and the
749 concentration of inhibitor which causes 50 per cent inhibition (I50) of an enzymatic reaction.
750 Biochem Pharmacol 22:3099–3108.

751 37. Gans P, Sabatini A, Vacca A. 1996. Investigation of equilibria in solution. Determination of
752 equilibrium constants with the HYPERQUAD suite of programs. Talanta 43:1739–1753.

753 38. 2008. EUCAST definitive document EDef 7.1: method for the determination of broth
754 dilution MICs of antifungal agents for fermentative yeasts. Clin Microbiol Infect 14:398–
755 405.

756 39. 2008. EUCAST Technical Note on the method for the determination of broth dilution
757 minimum inhibitory concentrations of antifungal agents for conidia-forming moulds. Clin
758 Microbiol Infect 14:982–984.

759 40. Klepser ME, Ernst EJ, Lewis RE, Ernst ME, Pfaller MA. 1998. Influence of test conditions
760 on antifungal time-kill curve results: Proposal for standardized methods. Antimicrob Agents
761 Chemother 42:1207–1212.

762 41. Cowen LE, Sanglard D, Calabrese D, Sirjusingh C, Anderson JB, Kohn LM. 2000. Evolution
763 of drug resistance in experimental populations of Candida albicans. JBacteriol 182:1515–
764 1522.

765 42. Livak KJ, Schmittgen TD. 2001. Analysis of Relative Gene Expression Data Using Real-

766 Time Quantitative PCR and the 2−ΔΔCT Method. Methods 25:402–408.

767 43. Scudiero D a, Shoemaker RH, Paull KD, Scudiere D a, Paul KD, Monks A, Tierney S,
768 Nofziger TH, Currens MJ, Seniff D, Boyd MR. 1988. Evaluation of a Soluble Tetrazolium /
769 Formazan Assay for Cell Growth and Drug Sensitivity in Culture Using Human and Other
770 Tumor Cell Lines. Cancer Res 48:4827–4833.

771 44. MacCallum DM. 2012. Mouse intravenous challenges models and applications. Methods
772 Mol Biol 845:499–509.

773

774

Figure 1. A) Structures of the compounds ZAC307, ZAC989, ZAC623, TPEN and EDTA. B) Abbreviated synthetic pathway for ZAC307: [a], i) *N*-Methylmethanamine, TEA, 2-propanol, 0 °C, 2h, evaporated, ii) Hydrazine hydrate, reflux (block temp 120 °C), 2h, 65%; [b], 2-propanol, reflux, 1h, 69%. C) Abbreviated synthetic pathway for ZAC989: [a], NaH, abs. THF, 0 °C, 3h, NH_4Cl, 82%; [b], Diethylether, 0 °C , conc. HCl, quant. ; [c], Load onto SCX in methanol, elute with 1M NH_3 in MeOH, 95%; [d], 2-propanol, reflux 90 min, 14%; [e], NMP, DIPEA, 30 min at 100 °C, 89%. D) Abbreviated synthetic pathway for ZAC623: [a], *tert*-Butyl-*N*-aminocarbamate, DIPEA, THF, rt → reflux, 98%; [b], 3-[(3S)-pyrollidin—3-yl]oxypyridine-4-carbonitrile (see B) reac. c), DIPEA, NMP, 120 ^{0}C , 1h, 71%. ; [c], i) TFA, DCM, rt, 30 min, ii) Load onto SCX in methanol, elute with 0.5M NH_3 in MeOH, quant. ; [d], Z-3-amino-but-2-enenitrile, AcOH, EtOH, 80 °C 4h, 85%.

Figure 2. Potentiometric titration results for ZAC307 and ZAC989. A) Potentiometric equilibrium curves of ZAC307 in the absence or presence of 0.5 mole equivalent of $Zn(NO_3)_2$, $CaCl_2$ or $MgCl_2$ in DMSO/water (70:30 v/v). B) Potentiometric equilibrium curves of ZAC989 in the absence or presence of 0.5 mole equivalent of $Zn(CF_3SO_3)_2$, $CuSO_4$, $CaCl_2$ or $MgCl_2$ in DMSO/water (70:30 v/v). C, D and E) Species distribution diagram as a function of pH for a system containing C) 0.5 mM Zn(II) and 1 mM ZAC307, D) 0.5 mM Zn(II) and 1 mM ZAC989 and E) 0.5 mM Cu(II) and 1 mM ZAC989.

Figure 3. A) *Candida albicans* growth inhibition by ZAC989 and ZAC307, but not by the close analogous compound ZAC623. B) *Candida albicans* growth inhibition by EDTA and TPEN. C+D) Abrogation of the antifungal effect of ZAC989 and ZAC307 in *Candida albicans* cells was achieved by the addition of Zn^{2+} or Cu^{2+} ions. The graphs display how much (µM) Zn^{2+}, Cu^{2+}, Fe^{2+},

798 Mg^{2+} or Ca^{2+} is required to abrogate the antifungal effects of 1.8 µg/mL ZAC989 or 1.4 µg/mL
799 ZAC307. *C. albicans* growth (expressed as %) in A-D was normalized to *C. albicans* growth in
800 RPMI containing 1.5 % DMSO. Graphs represent mean ± SEM for 2-3 independent experiments.
801
802 **Figure 4.** A) Time-kill experiments with *C. albicans* revealed that ZACs exhibit fungistatic activity.
803 The following final concentrations of compound were applied; 0.5 µg/mL amphotericin B (AMB),
804 3.6 µg/mL ZAC989; 4.4 µg/mL EDTA; 4.2 µg/mL TPEN. Data shows the mean ± SEM for two
805 biological replicates. B and C) *C. albicans* cells exposed to ZAC989 and ZAC307 for 5 days
806 resume normal growth (B), while cells exposed to TPEN for 5 days show poor recovery (C). *C.*
807 *albicans* cells exposed to EDTA resumed visible growth after 48 h of compound incubation
808 (concentration range 0.22 µg/mL to 22 µg/mL) and were therefore not evaluated for MFC. D)
809 Decrease in intracellular zinc as evidenced by a decrease in zinbo-5 fluorescence signal suggests
810 that ZAC989 and ZAC307 act intracellularly in *C. albicans*. The following final concentrations of
811 compound was applied: 9 µg/mL ZAC989, 7 µg/mL ZAC307, 15 µg/mL EDTA, 1.3 µg/mL TPEN.
812 Data shows the mean ± SEM for two biological replicates. E) Resistance induction study; no change
813 in the MIC for the ZACs after repeated ZAC exposure, while a significant increase in the MIC was
814 observed for *C. albicans* after 22 passages with repeated exposure to fluconazole (FLC) (1.0
815 µg/mL).
816
817 **Figure 5.** Effect of ZAC307 and ZAC989 on the growth capacity of several *A. fumigatus* strains.
818 (A) The wild-type AF14 strain was cultured in 24-well culture plates inoculated with 10^5 conidia
819 per well in a total volume of culture media of 1 mL. Not inoculated (Ni) culture media were used as
820 background reference. Media were not supplemented with zinc or were supplemented with 2, 5 or
821 50 µM $ZnSO_4$ in the absence (–) or the presence (+) of ZAC307 (Z7) or ZAC989 (Z9), as indicated.

822 Plates were incubated a 37 ºC in a humid atmosphere for 44 h, scanned, quantified and the growth
823 was represented graphically. (B) Effect of ZACs on the growth capacity of the Δ*zrfA*Δ*zrfB* mutant
824 strain (AF48). (C) Effect of ZACs on the growth capacity of the Δ*zrfA*Δ*zrfB*Δ*zrfC* mutant strain
825 (AF721). (D) Effect of ZACs on the growth capacity of the Δ*zrfA*Δ*zrfB*Δ*zrfC*[*zrfC*] mutant strain
826 (AF731). (E) Effect of ZACs on the growth capacity of the Δ*zrfC* mutant strain (AF54). The AF48,
827 AF721, AF731 and AF54 strains were all cultured and incubated in 24-well culture plates and their
828 growth were quantified as described for the wild-type strain. In all cases the relative arbitrary units
829 obtained after quantification of the plates were normalized by taking the average of the background
830 values of not inoculated cultures as a growth capacity of 0 % and the growth reached by the wild-
831 type strain in media supplemented with 50 µM zinc in the absence of ZACs as a growth capacity of
832 100%. In all graphs, the data represent the average and standard deviation of two independent
833 experiments in which all strains had been cultivated in duplicate.
834
835 **Figure 6.** Effect of the ZACs, the extracellular chelator EDTA and the intracellular chelator TPEN
836 on the transcription of ZafA target genes under zinc-limiting conditions. The wild-type strain pre-
837 cultured in the sRPMI zinc-limiting medium for 20 h at 37 ºC with shaking at 200 rpm was
838 untreated (–Zn) or treated with 20 µM zinc (+Zn), 21 µg/mL ZAC307 (+ZAC307), 27 µg/mL
839 ZAC989 (+ZAC989), 146 µg/mL EDTA (+EDTA) and 10.6 µg/mL TPEN (+TPEN). The
840 expression level of the indicated genes was analyzed by RT-qPCR using 18rRNA as an internal
841 reference. The changes in the relative expression ratios (rER) were measured after 2 h of incubation
842 following the treatment with the different compounds and compared to the expression levels
843 observed under zinc-limiting conditions (–Zn). The bar diagram depicts the average and standard
844 deviation of the results obtained in two independent experiments.
845

Figure 7. *In vivo* efficacy data for ZAC989 and ZAC307 in a 3-day candidiasis kidney burden model. Dosing with and without pre-treatment (day -1) yields the same CFU reduction for ZAC307. # Indicates no pre-treatment in this arm. * p <0.05 compared to infected untreated control group, one-way ANOVA.

Table 1: Dissociation constant (K_D) determination between chelating compounds and zinc. K_D determination for the compound-Zn^{2+} complex was performed with a fluorescence-based competition assay using fluozin-3.

Compound	Compound-Zn^{2+} K_D (µM)
ZAC989	0.013
ZAC307	0.071
ZAC623	>6
EDTA	<0.01
TPEN	<0.01

862 **Table 2.** Determination of the minimum inhibitory concentration (MIC) of several different
863 *Candida* species.

Fungal growth inhibition of *Candida* spp. Minimum inhibitory concentration (MIC; µg/mL)						
Compound	*C. albicans* SC5314	*C. parapsilosis* ATCC 22019	*C. glabrata* ATCC 90030	*C. glabrata* Cg003[a]	*C. tropicalis* Ct016	*C. krusei* ATCC 6258
ZAC989	0.6	0.8	0.9	0.6	0.9	0.8
ZAC307	0.4	0.4	0.2	0.2	0.4	0.4
ZAC623	>54	>54	ND	ND	ND	>54

864 [a] This *Candida glabrata* strain has mutations resulting in increased efflux pump activity as
865 compared to wild type isolates (34). ND: Not determined.

866

867 **Table 3.** Minimum inhibitory concentration (MIC) determination of several different *Aspergillus*
868 and mucorales species.

Fungal growth inhibition of mold isolates Minimum inhibitory concentration (MIC; µg/mL)						
Compound	*Aspergillus fumigatus* ATCC 13073	*Aspergillus flavus* ATCC 15547	*Aspergillus terreus* At070	*Rhizopus oryzae* ATCC 34965	*Rhizopus microspores* ATCC 66276	*Mucor indius* ATCC MYA-4678
ZAC989	5.4	5.1	1.6	1.7	0.5	1.1
ZAC307	4.0	1.3	1.3	1.3	0.4	1.3

869 **Table 4.** Selected genes for quantifying their relative expression level by RT-qPCR

Regulation by ZafA	Gene	Code	Function
Regulated	*zafA*	AFUA_1G10080	Major transcriptional regulator of zinc homeostasis
	zrfB	AFUA_2G03860	Zinc transporter of the ZIP family putatively located in the cytoplasmic membrane
	zrfC	AFUA_4G09560	Zinc transporter of the ZIP family putatively located in the cytoplasmic membrane
	zrfF	AFUA_2G08740	Zinc transporter of the ZIP family putatively located in vacuolar membrane
	zrcA	AFUA_7G06570	Zinc transporter of the CDF family putatively located in vacuolar membrane
	mchC	AFUA_8G02620	Putative zinc-metallochaperone
	sarA	AFUA_7G06810	Putative L-amino acid oxidase
Not regulated	*actA*	AFUA_6G04740	Actin
	tubB1	AFUA_1G10910	β-tubuline subunit 1
	gdpA	AFUA_5G01970	Glyceraldehyde-3-phosphate dehydrogenase
	pmaA	AFUA_3G07640	Plasma membrane H^+-ATPase
	mchA	AFUA_2G11720	Putative metallochaperone
	mchB	AFUA_4G07990	Putative metallochaperone

870

871

872

873 **Table 5.** Primers used to quantify mRNA by RT-qPCR.

Oligonucleotide	Sequence (5′ → 3′)
18SRNA-D	TGTTAAACCCTGTCGTGCTG
18SRNA-R	GTACAAAGGGCAGGGACGTA
ZAFA- D1	GGCAAGTCATTTACCGACAGC
ZAFA-R1	TCGATGACTTGACATGTTGGACG
ZRFB-D	ACCGGCAGAAGAAGCATTGA
ZRFB-R	ACCGCATCACCATCAACTCA
ZRFC-D	CAAACTCTCGGTGCTCGTCA
ZRFC-R	GAAGACAATCACCACCAGCA
qZRFF2-D	CGTATTCCCTCTCATGTCGTCG
qZRFF2-R	AGAGCCATTTGCCTGGTTCG
SARA-D	GCATATCATGTCACCGAGCACA
SARA-R	AGCCCCAACTCCAACAACAA
qMCHC-D	CATGCTAACGATGGGATGCG
qMCHC-R	CTTCGGTCTCCCAATGGTGG
qZRCA-D	TGCAGAGTGTTCCTCTCGGAGTCG
qZRCA-R	TCGCCAGATATGCAGTTCATGGACG
qACT3-D	CCACGTCACCACTTTCAACTCCATC
qACT3-R	TCCTTCTGCATACGGTCGGAGATAC
qGDPA2-D	CTCACTTGAAGGGTGGTGCC
qGDPA2-R	GATGTCGGAGGTGTAGGTGG
qPMA12-D	AGATCGCTACTCCTGAGCACG
qPMA12-R	CTTCTGCTCGGCAAGGTAAGC
BTUB-D	AACAACATCCAGACCGCTCT
BTUB-R	TGATCACCGACACGCTTGAA
qMCHA-D	GAAACCGCAACGAGCCATAC
qMCHA-R	ACGAGATCCGCCTTGTTCAG
qMCHB-D	TGATCTTGAGGTGCAGACGC
qMCHB-R	TGATGGTCATCCGTCAACCG

874

Antimicrobial Agents and Chemotherapy

875 **Table 6.** *In vitro* cell proliferation assay in HepG2.

Compound	HepG2 EC_{50} (24 h) µg/mL	HepG2 EC_{50} (72 h) µg/mL
ZAC989	>36	6.9 ±0.7
ZAC307	>28	13.2 ±0.8
EDTA	>29	>29
TPEN	1.6 ±0.2	1.4 ±0.8

876

877 **Table 7.** Fungal kidney burden candidiasis *in vivo* model

	Antifungal therapy				
	Untreated control	Fluconazole 3 mg/kg	ZAC989 60 mg/kg	ZAC307 60 mg/kg	ZAC307 60 mg/kg No pre-treatment
Mean log CFU/kidney	5.79 ±0.14	3.02 ±0.22	4.09 ±0.31	4.73 ±0.19	4.77 ±0.19
Mean log CFU/kidney reduction	NA	2.78*	1.71*	1.06*	1.03*

878 *p<0.05 compared to infected vehicle control group, one-way ANOVA

879 NA: not applicable

880

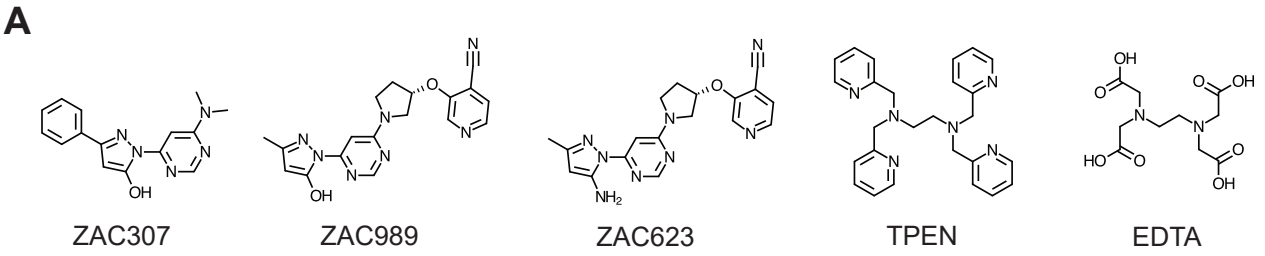

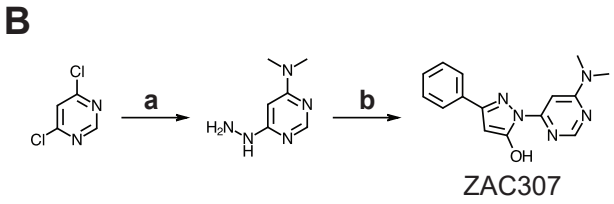

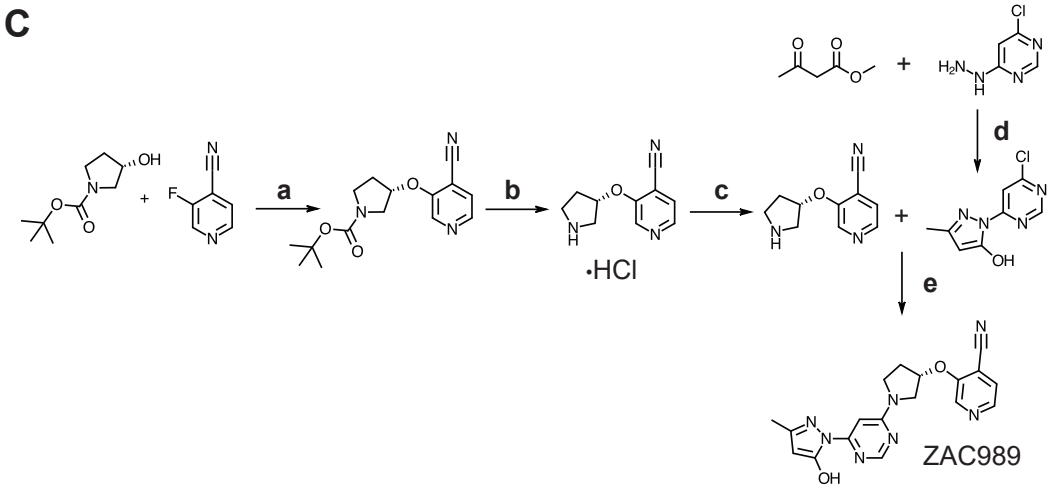

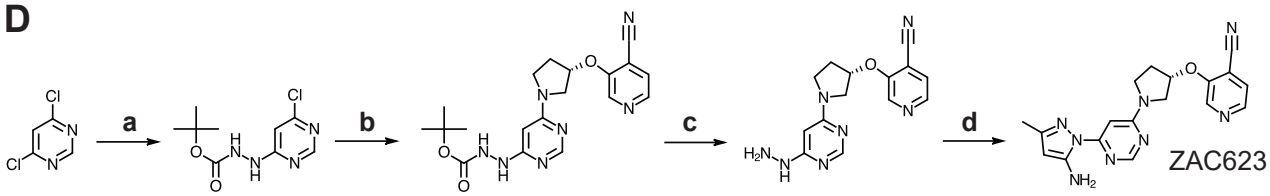

Antimicrobial Agents and Chemotherapy

Figure 1. A) Structures of the compounds ZAC307, ZAC989, ZAC623, TPEN and EDTA. B) Abbreviated synthetic pathway for ZAC307: [a], i) *N*-Methylmethanamine, TEA, 2-propanol, 0 °C, 2h, evaporated, ii) Hydrazine hydrate, reflux (block temp 120 °C), 2h, 65%; [b], 2-propanol, reflux, 1h, 69%. C) Abbreviated synthetic pathway for ZAC989: [a], NaH, abs. THF, 0 °C, 3h, NH_4Cl, 82%; [b], Diethylether, 0 °C , conc. HCl, quant. ; [c], Load onto SCX in methanol, elute with 1M NH_3 in MeOH, 95%; [d], 2-propanol, reflux 90 min, 14%; [e], NMP, DIPEA, 30 min at 100 °C, 89%. D) Abbreviated synthetic pathway for ZAC623: [a], *tert*-Butyl-*N*-aminocarbamate, DIPEA, THF, rt → reflux, 98%; [b], 3-[(3S)-pyrollidin—3-yl]oxypyridine-4-carbonitrile (see B) reac. c), DIPEA, NMP, 120 °C , 1h, 71%. ; [c], i) TFA, DCM, rt, 30 min, ii) Load onto SCX in methanol, elute with 0.5M NH_3 in MeOH, quant. ; [d], Z-3-amino-but-2-enenitrile, AcOH, EtOH, 80 °C 4h, 85%.

Antimicrobial Agents and Chemotherapy

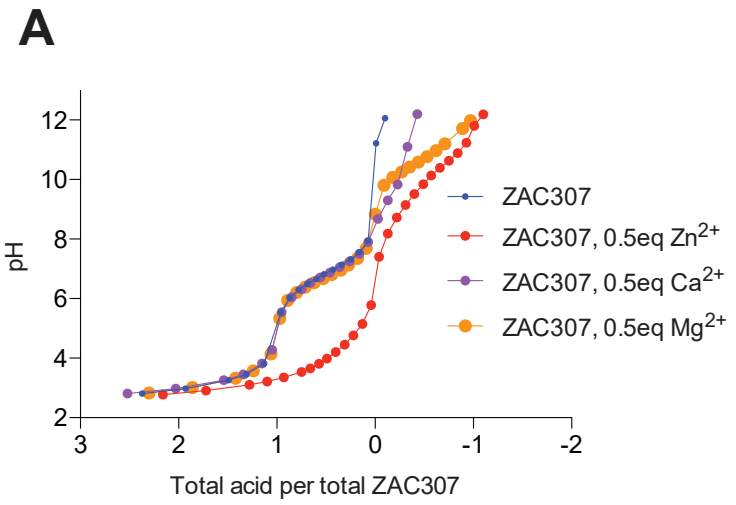

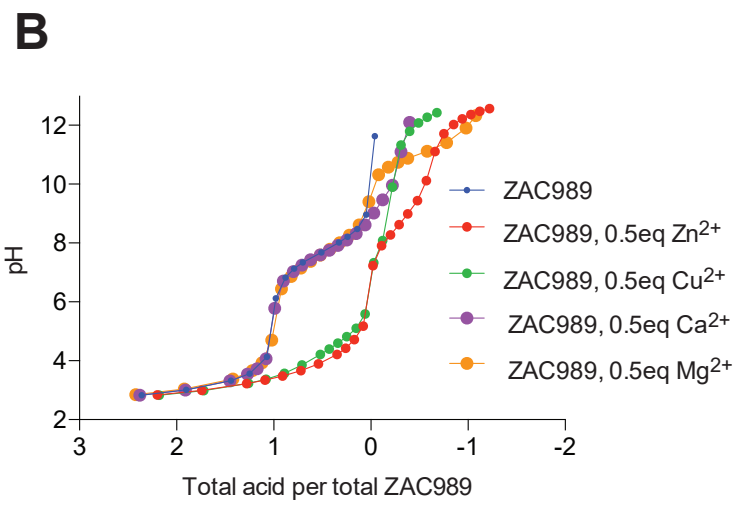

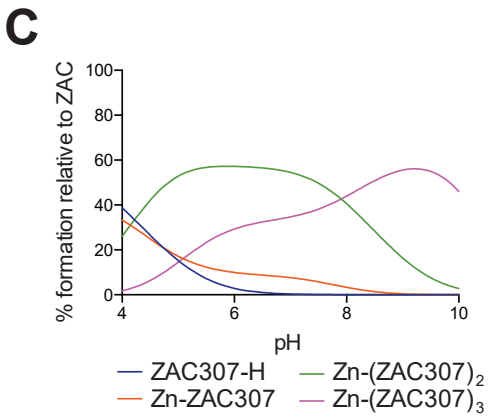

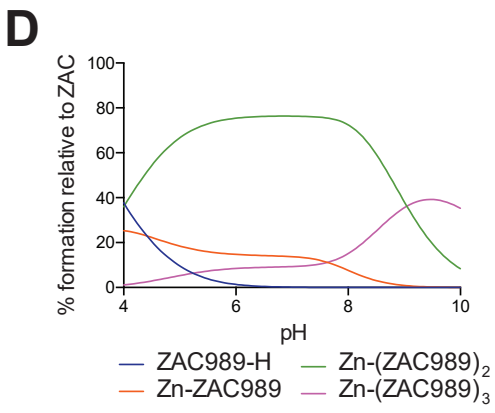

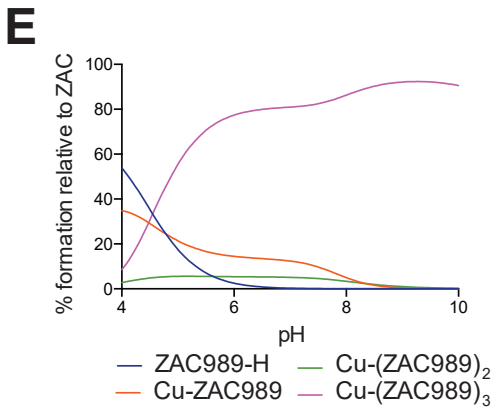

Figure 2. Potentiometric titration results for ZAC307 and ZAC989. A) Potentiometric equilibrium curves of ZAC307 in the absence or presence of 0.5 mole equivalent of $Zn(NO_3)_2$, $CaCl_2$ or $MgCl_2$ in DMSO/water (70:30 v/v). B) Potentiometric equilibrium curves of ZAC989 in the absence or presence of 0.5 mole equivalent of $Zn(CF_3SO_3)_2$, $CuSO_4$, $CaCl_2$ or $MgCl_2$ in DMSO/water (70:30 v/v). C, D and E) Species distribution diagram as a function of pH for a system containing C) 0.5 mM Zn(II) and 1 mM ZAC307, D) 0.5 mM Zn(II) and 1 mM ZAC989 and E) 0.5 mM Cu(II) and 1 mM ZAC989.

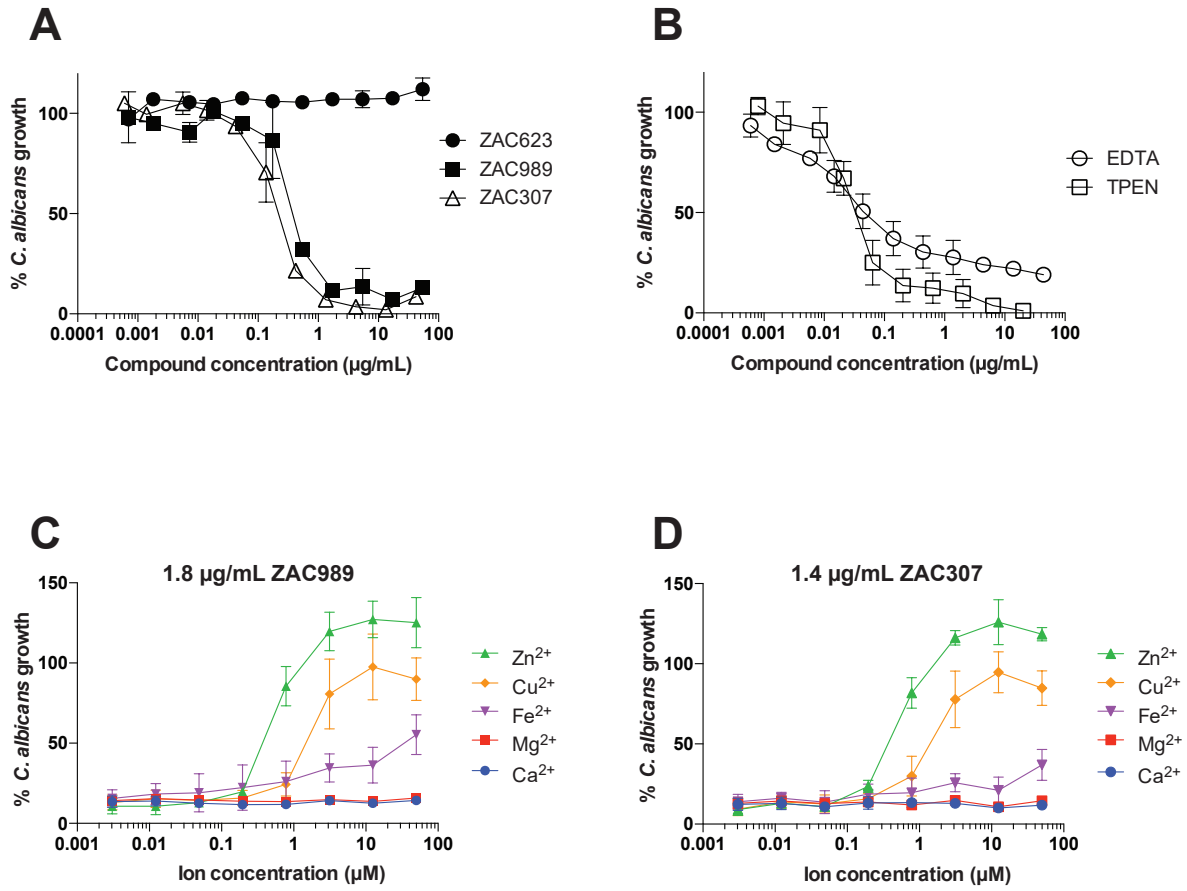

Figure 3. A) *Candida albicans* growth inhibition by ZAC989 and ZAC307, but not by the close analogous compound ZAC623. B) *Candida albicans* growth inhibition by EDTA and TPEN. C+D) Abrogation of the antifungal effect of ZAC989 and ZAC307 in *Candida albicans* cells was achieved by the addition of Zn^{2+} or Cu^{2+} ions. The graphs display how much (μM) Zn^{2+}, Cu^{2+}, Fe^{2+}, Mg^{2+} or Ca^{2+} is required to abrogate the antifungal effects of 1.8 μg/mL ZAC989 or 1.4 μg/mL ZAC307. *C. albicans* growth (expressed as %) in A-D was normalized to *C. albicans* growth in RPMI containing 1.5 % DMSO. Graphs represent mean ±SEM for 2-3 independent experiments.

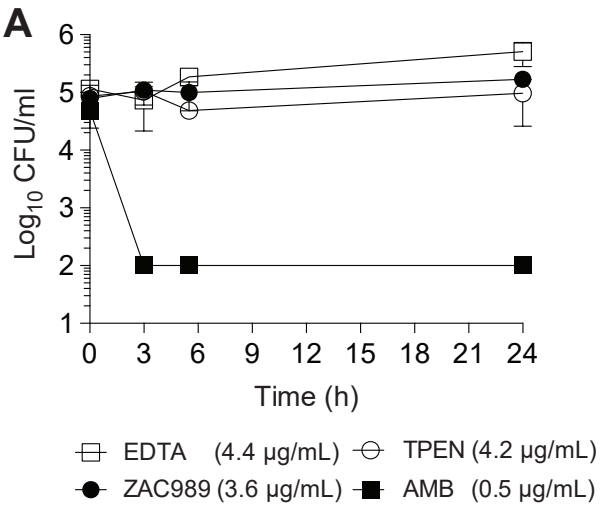

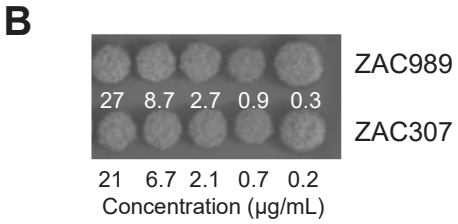

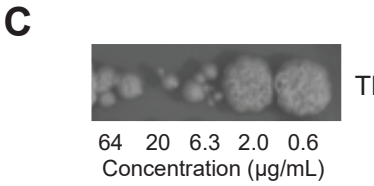

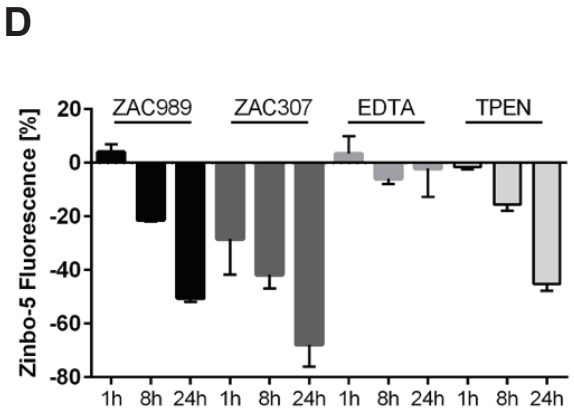

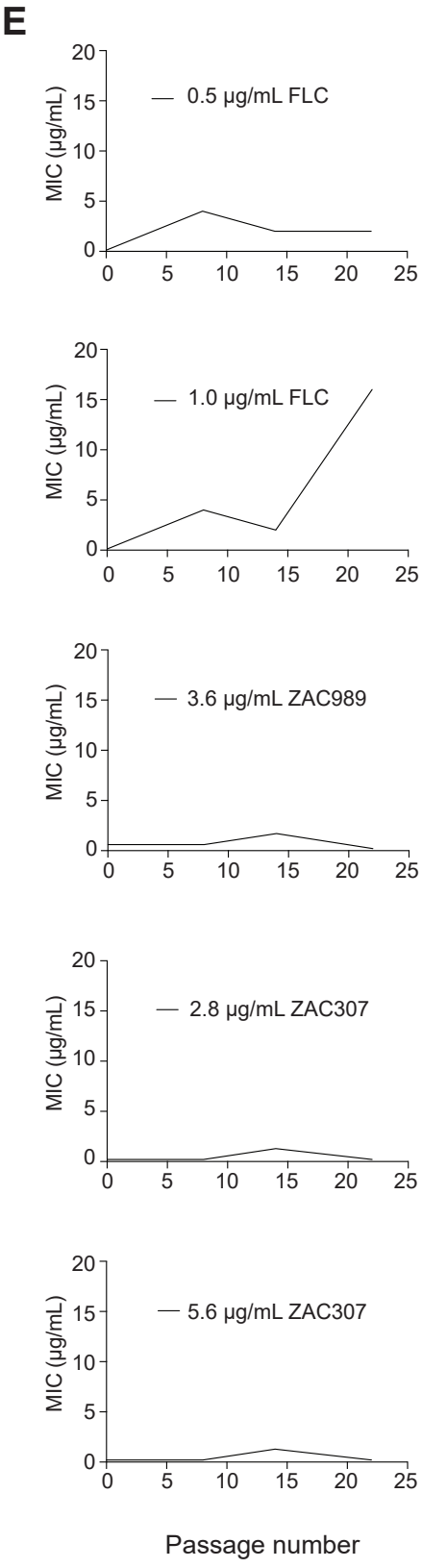

Figure 4. A) Time-kill experiments with *C. albicans* revealed that ZACs exhibit fungistatic activity. The following final concentrations of compound were applied; 0.5 µg/mL amphotericin B (AMB), 3.6 µg/mL ZAC989; 4.4 µg/mL EDTA; 4.2 µg/mL TPEN. Data shows the mean ± SEM for two biological replicates. B and C) *C. albicans* cells exposed to ZAC989 and ZAC307 for 5 days resume normal growth (B), while cells exposed to TPEN for 5 days show poor recovery (C). *C. albicans* cells exposed to EDTA resumed visible growth after 48 h of compound incubation (concentration range 0.22 µg/mL to 22 µg/mL) and were therefore not evaluated for MFC. D) Decrease in intracellular zinc as evidenced by a decrease in zinbo-5 fluorescence signal suggests that ZAC989 and ZAC307 act intracellularly in *C. albicans*. The following final concentrations of compound was applied: 9 µg/mL ZAC989, 7 µg/mL ZAC307, 15 µg/mL EDTA, 1.3 µg/mL TPEN. Data shows the mean ± SEM for two biological replicates. E) Resistance induction study, no change in the MIC for the ZACs after repeated ZAC exposure, while a significant increase in the MIC was observed for *C. albicans* after 22 passages with repeated exposure to fluconazole (FLC) (1.0 µg/mL).

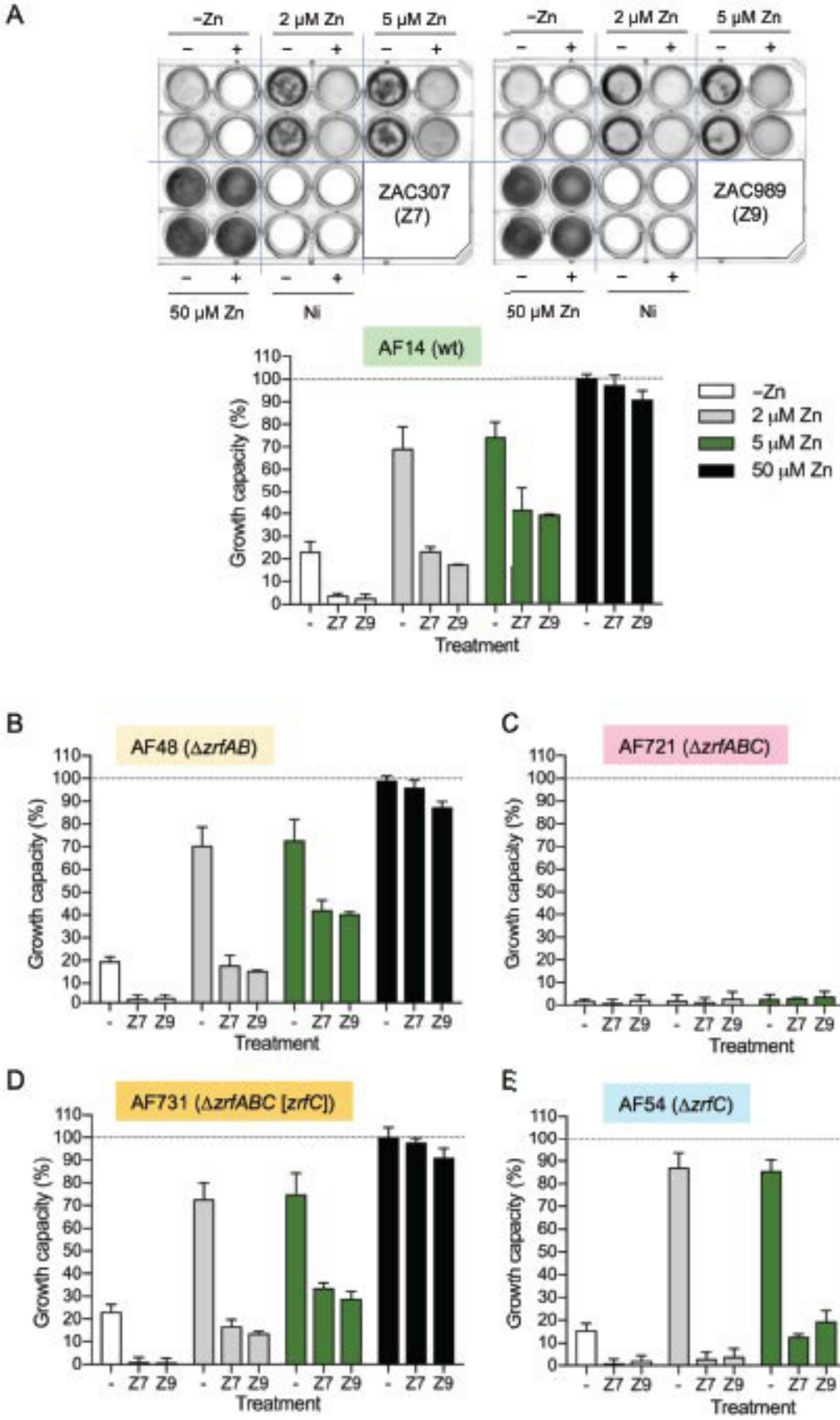

Figure 5. Effect of ZAC307 and ZAC989 on the growth capacity of several *A. fumigatus* strains. (A) The wild-type AF14 strain was cultured in 24-well culture plates inoculated with 10^5 conidia per well in a total volume of culture media of 1 mL. Not inoculated (Ni) culture media were used as background reference. Media were not supplemented with zinc or were supplemented with 2, 5 or 50 µM $ZnSO_4$ in the absence (–) or the presence (+) of ZAC307 (Z7) or ZAC989 (Z9), as indicated. Plates were incubated a 37 °C in a humid atmosphere for 44 h, scanned, quantified and the growth was represented graphically. (B) Effect of ZACs on the growth capacity of the Δ*zrfA*Δ*zrfB* mutant strain (AF48). (C) Effect of ZACs on the growth capacity of the Δ*zrfA*Δ*zrfB*Δ*zrfC* mutant strain (AF721). (D) Effect of ZACs on the growth capacity of the Δ*zrfA*Δ*zrfB*Δ*zrfC*[*zrfC*] mutant strain (AF731). (E) Effect of ZACs on the growth capacity of the Δ*zrfC* mutant strain (AF54). The AF48, AF721, AF731 and AF54 strains were all cultured and incubated in 24-well culture plates and their growth were quantified as described for the wild-type strain. In all cases the relative arbitrary units obtained after quantification of the plates were normalized by taking the average of the background values of not inoculated cultures as a growth capacity of 0 % and the growth reached by the wild-type strain in media supplemented with 50 µM zinc in the absence of ZACs as a growth capacity of 100 %. In all graphs, the data represent the average and standard deviation of two independent experiments in which all strains had been cultivated in duplicate.

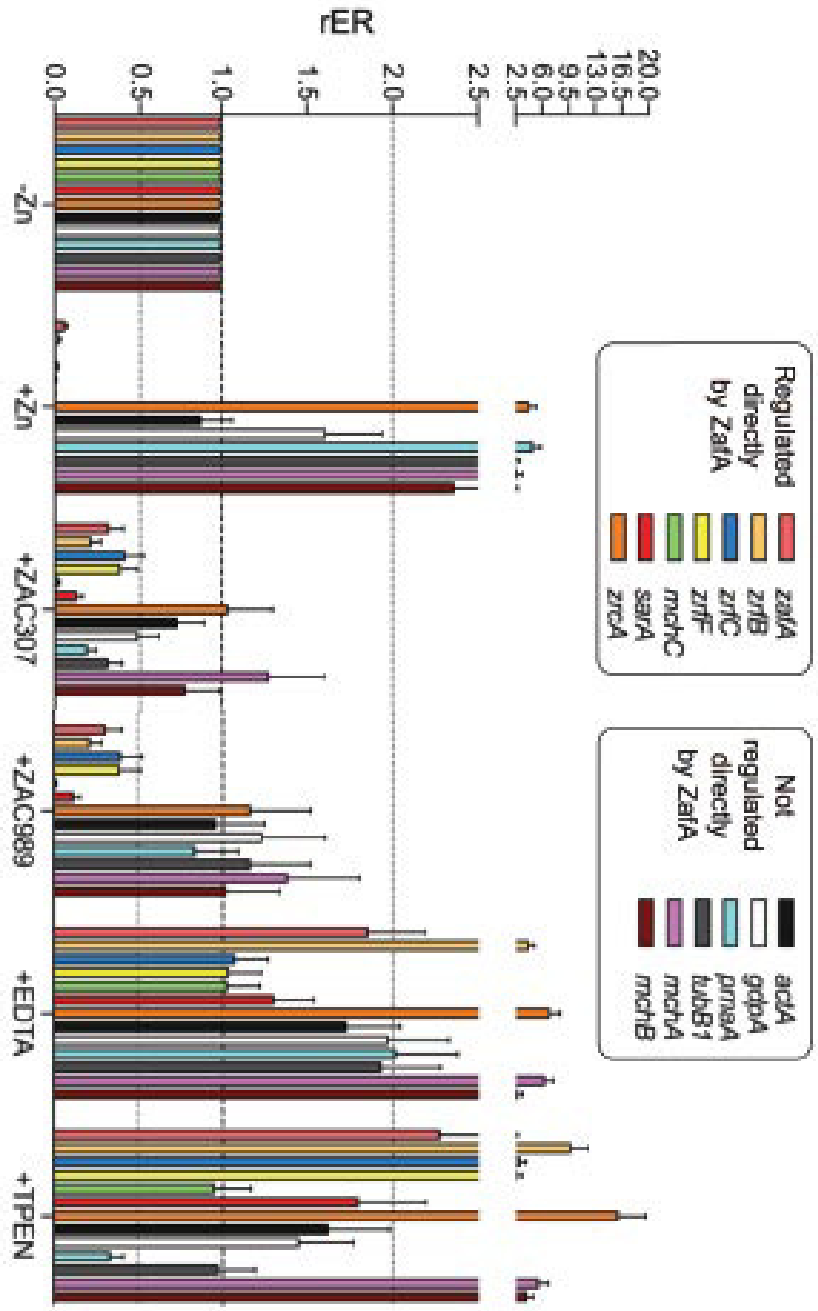

Figure 6. Effect of the ZACs, the extracellular chelator EDTA and the intracellular chelator TPEN on the transcription of ZafA target genes under zinc-limiting conditions. The wild-type strain pre-cultured in the sRPMI zinc-limiting medium for 20 h at 37 °C with shaking at 200 rpm was untreated (–Zn) or treated with 20 µM zinc (+Zn), 21 µg/mL ZAC307 (+ZAC307), 27 µg/mL ZAC989 (+ZAC989), 146 µg/mL EDTA (+EDTA) and 10.6 µg/mL TPEN (+TPEN). The expression level of the indicated genes was analyzed by RT-qPCR using 18rRNA as an internal reference. The changes in the relative expression ratios (rER) were measured after 2 h of incubation following the treatment with the different compounds and compared to the expression levels observed under zinc-limiting conditions (–Zn). The bar diagram depicts the average and standard deviation of the results obtained in two independent experiments.

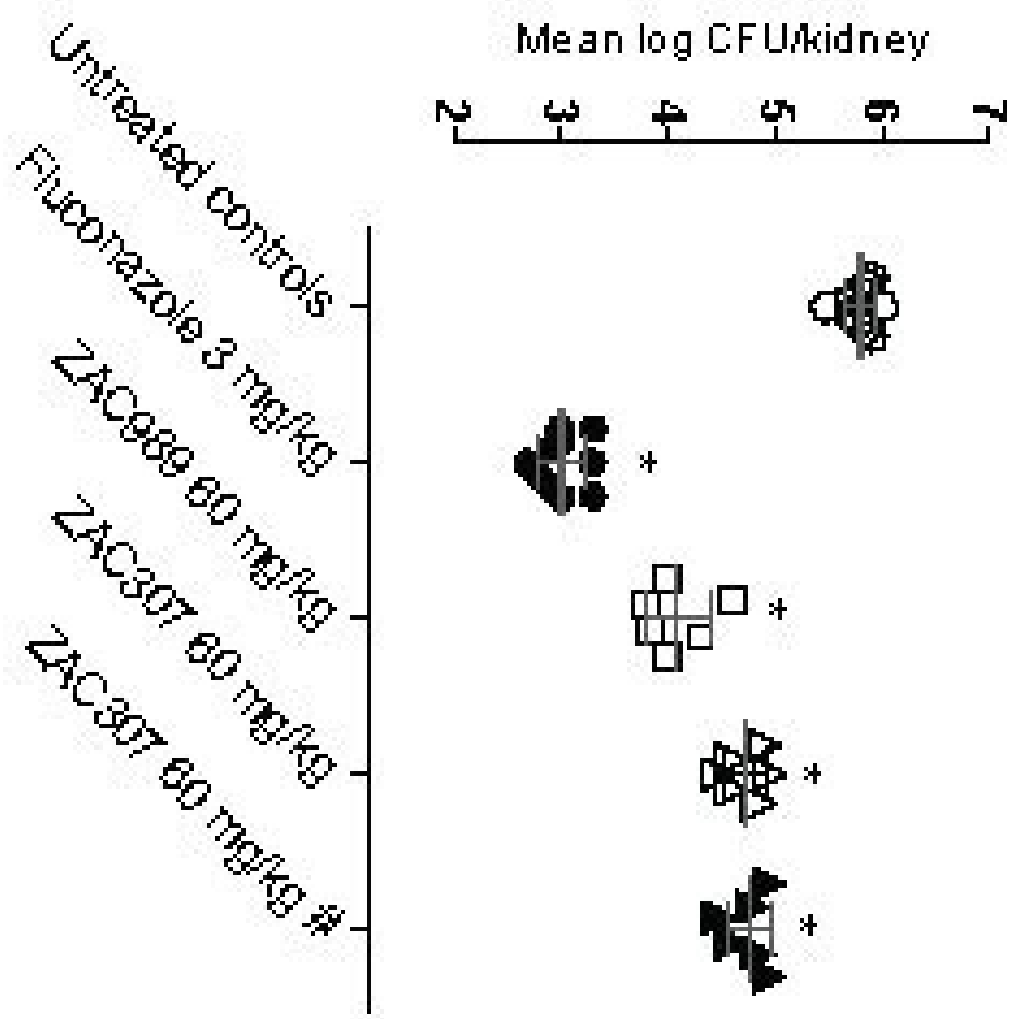

Figure 7. *In vivo* efficacy data for ZAC989 and ZAC307 in a 3-day candidiasis kidney burden model. Dosing with and without pre-treatment (day -1) yields the same CFU reduction for ZAC307. # Indicates no pre-treatment in this arm. * $p < 0.05$ compared to infected untreated control group, one-way ANOVA.

Antimicrobial Agents and Chemotherapy